

Feeding performance of the marine calanoid copepod *Temora longicornis*

Student: Hans van Someren Gréve
Student number: 0346535
E-mail: h.vansomerengreve@students.uu.nl
Supervisors Denmark Technical University: Prof. Thomas Kiørboe
Dr. Rodrigo J. Gonçalves
Supervisor Utrecht University: Dr. Aat Barendregt
Date: August 5th, 2013

Master thesis Sustainable Development, track GCE (30 ECTS) – Utrecht University



TABLE OF CONTENTS

1. BACKGROUND OF RESEARCH	3
1.1 Introduction	3
1.2 Copepod feeding	4
1.2.1 The effect of prey concentration on copepod feeding: the functional response	6
1.2.2 The effect of prey size on copepod feeding: prey size spectrum	7
2. PROBLEM DEFINITION AND AIM	9
3. RESEARCH QUESTIONS	9
4. HYPOTHESES	10
5. METHODS	11
5.1 Experimental design	11
5.2 Data analysis	12
5.2.1 Calculation of prey concentration, clearance and ingestion rates	12
5.2.2 Fitting the functional response model	13
5.2.3 Comparative analysis	14
6. RESULTS	15
6.1 The effect of prey concentration on ingestion and clearance rate	15
6.2 The effect of prey size on ingestion and clearance rate	20
6.2.1 The effect of prey size on ingestion rate	20
6.2.2 The effect of prey size on clearance rate	21
7. DISCUSSION	23
7.1 The effect of prey concentration on the ingestion and clearance rate	23
7.1.1 Prey density dependant ingestion and clearance rate	23
7.1.2 Fitting the functional response model	23
7.2 The effect of prey size on ingestion and clearance rate	24
7.2.1 The effect of prey size on the ingestion rate	24
7.2.2 The effect of prey size on the clearance rate	25
7.3 The feeding performance of <i>T. longicornis</i> compared to other marine copepods	26
7.4 Complications in modeling copepod feeding	27
8. CONCLUSION	28

REFERENCES

APPENDIX I Results of bottle incubation experiments and statistical analysis of observations

APPENDIX II Dataset clearance and ingestion rates marine copepods from literature

Cover picture shows the adult female *T. longicornis*. Original picture from Sars (1901).

1. BACKGROUND OF RESEARCH

1.1 Introduction

Among many of the chemical elements and compounds in ecosystems there is a continuous exchange between organisms and the environment. The pathway by which chemical elements and compounds move through the abiotic (lithosphere, atmosphere and hydrosphere) and biotic (biosphere) reservoirs are called biogeochemical cycles (Harvey, 2000; Nybakken, 2001). Forcing of the nutrient and carbon biochemical cycle by anthropogenic activities has turned eutrophication and global change into key issues in marine research. Good knowledge of sources and sinks is necessary in order to understand the nutrient and carbon cycle (Frangoulis et al., 2005). The carbon cycle is one of the most important biogeochemical cycles, because it is not only vital to the continued maintenance of life, but also critically important to climate regulation (Harvey, 2000; Nybakken, 2001).

The oceans are most likely to be an important long term sink for anthropogenic released carbon (Harvey, 2000; Sabine et al., 2004). As atmospheric CO₂ enters the ocean's surface layer it is transferred to deeper waters via a physical pathway (the solubility pump, where carbon is transported to deep water via convection) and two biological pathways (the carbonate pump and biological CO₂ pump where biogenic particles are actively or passively vertically transported) (Harvey, 2000; Frangoulis et al., 2005).

Marine zooplankton, feeding on particulate organic matter including phytoplankton, plays a key role in the biological CO₂ pump (Frangoulis et al., 2005; Buesseler and Lampitt, 2008). Marine phytoplankton produce organic matter from dissolved carbon and nutrients in the ocean's surface layer using solar energy and is responsible for 95 % of the oceans primary production and for 38 % of the total primary production on Earth (Duarte and Cebrian, 1996). In the marine food web they provide larger plankton, such as zooplankton, food which in turn are eaten by larger organisms. Although marine zooplankton is relatively small (μm to mm size scale), their estimated total biomass is larger than that of other consumers (Frangoulis et al., 2005). As primary grazers of phytoplankton they consume more than 40% of the phytoplankton production (Duarte and Cebrian, 1996) and release dissolved carbon to their environment through excretion and respiration and particulate carbon in the form of detritus (faecal pellets, dead eggs, moults and carcasses) (i.e. Frangoulis et al., 2005). The release of dissolved carbon to the environment makes it available for autotrophic and mixotrophic organisms and can be seen as recycling of carbon in euphotic zone. The particulate carbon flux can be seen as vertical transport of carbon to the deeper ocean (Frangoulis et al., 2005) that links the atmospheric CO₂ sink to the deeper ocean carbon sink where carbon is sequestered for longer time scales (Buesseler and Lampitt, 2008). The production of faecal pellets by zooplankton plays the most important role in this vertical transport of particulate carbon. It accelerates the vertical carbon flux by compaction and packing of phytoplankton organic matter that rapidly sinks out of the euphotic zone to the deep ocean (Frangoulis et al., 2005) where most the organic carbon is consumed and respired and where a small part is buried in the seafloor (Falkowski and Oliver, 2007). Fig. 1 shows the role of zooplankton in the ocean carbon cycle.

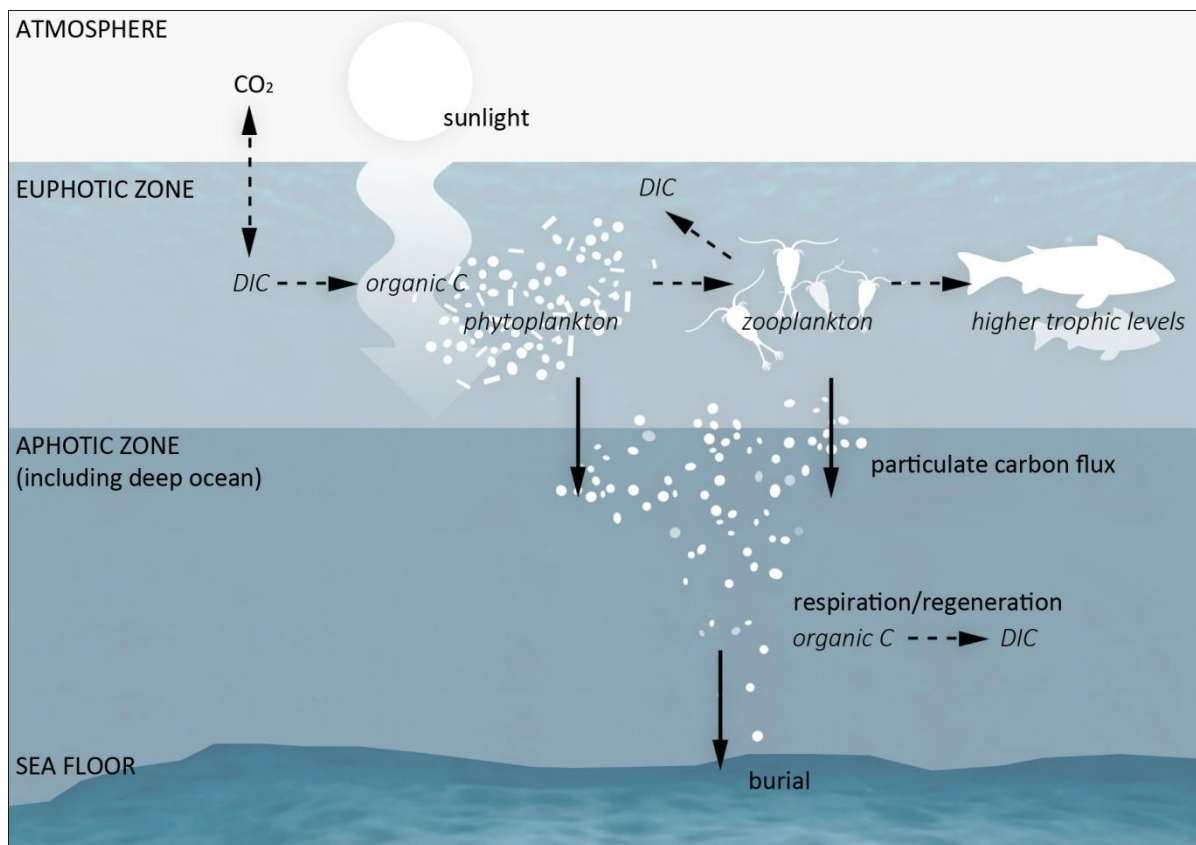


Fig. 1. The role of zooplankton in the cycling of carbon. There is a constant exchange between atmospheric carbon (CO_2) and carbon in the ocean's surface layer (DIC). In the sunlit euphotic zone (where photosynthesis is viable) phytoplankton fixes DIC into organic carbon. Zooplankton graze on phytoplankton transferring carbon to higher trophic levels and accelerates the particulate carbon flux to the deep ocean by faecal pellet production. A large fraction of the particulate carbon flux is regenerated into an inorganic form due to respiration and a small fraction is buried in the seafloor (based on Falkowski and Oliver, 2007 and Williams and Follows, 2011).

The feeding rate of zooplankton on phytoplankton is an important variable in the investigation of the role of zooplankton in the ocean carbon cycle, because it controls phytoplankton and zooplankton distribution (Anderson, 2010) and determines the strength of the carbon flux to the ocean carbon sink (Cox et al., 2000).

Zooplankton feeding rates are being used in complex marine ecosystem models to model the effect of zooplankton grazing on phytoplankton distribution (Anderson, 2010) or as part of the biological component of a ocean carbon-cycle model within a general circulation model (GCM), where feeding rate is not only used to model the regulation of phytoplankton by zooplankton grazing but also to model detritus formation and the downward flux of particulate carbon (Cox et al., 2000).

1.2 Copepod feeding

Within the plankton classification (Table 1) seven groups of plankton can be identified based on size. The three larger plankton groups (megaplankton, macroplankton and mesoplankton) are also referred to as the *net plankton* because these groups are usually captured in standard plankton nets. The net zooplankton throughout the world's oceans is dominated by the mesozooplankters of the subclass Copepoda (Nybakken, 2001). Copepods are a successful group and represent 80% of all mesozooplankters in terms of biomass (Kiørboe, 1998). They primarily graze larger phytoplankton

such as diatoms and dinoflagellates, especially in coastal waters (Nybakken, 2001). The small copepod *Temora longicornis* (Müller) (adult female prosome length is 0.52-1.40 mm (Conway, 2006)) is one of the most abundant copepod species in temperate saline waters of the northern hemisphere (Van Duren, 2000; Gentsch et al., 2009). They may have a substantial impact on the phytoplankton standing stock and play a major role in the North Sea food web throughout the year (Gentsch et al., 2009). In Long Island Sound (USA) the copepod is able to remove up to 34 % of the phytoplankton stock (Dam and Peterson, 1993). Fig. 2 shows some important characteristics of the marine copepod *T. longicornis*.

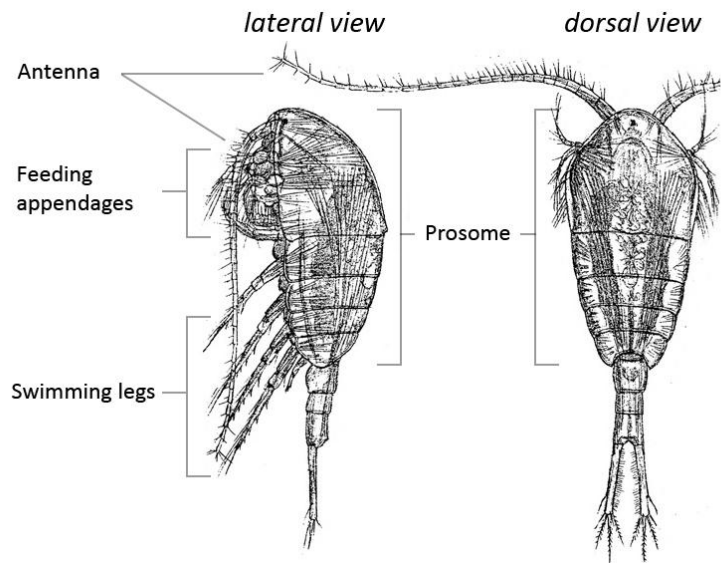


Fig. 2. Lateral and dorsal view of an adult female *Temora longicornis* (Sars, 1901).

Table 1. Size classification for plankton organisms (after Nybakken, 2001)

Class name	Size Class						
	Femtoplankton (0,02-0,2 μm)	Picoplankton (0,2-2,0 μm)	Nanoplankton (2,0-20 μm)	Microplankton (20-200 μm)	Mesoplankton (0,2-20 mm)	Macroplankton (2-20 cm)	Megaplankton (20-200 cm)
Viroplankton	■						
Bacterioplankton		■					
Mycoplankton			■				
Phytoplankton			■				
Protozooplankton			■				
Metazooplankton				■			
Size (m)	10 ⁻⁷	10 ⁻⁶	10 ⁻⁵	10 ⁻⁴	10 ⁻³	10 ⁻²	10 ⁻¹

The feeding rate of the copepod is often expressed as *ingestion rate* or as *clearance rate*. The ingestion rate is defined as the amount of food ingested per individual per time unit. The clearance rate is the volume of water cleared of food particles per unit time. This term however, should not imply that this volume of water has actually passed the feeding appendages of the copepod or that all suspended particles have been removed or consumed (Wetzel and Likens, 2003). High speed photography reveals the copepod feeds on phytoplankton by moving water with their feeding appendages past their body and uses its feeding appendages (second maxillae) to actively capture and filter water that contains food particles (Koehl and Strickler, 1981). Due to this feeding current, feeding and swimming are likely to be closely linked (Van Duren, 2000). The copepods feeding behavior depends on various factors such as prey concentration and size, prey quality (Fernandez, 1979), prey type (DeMott and Watson, 1991) time of the day, temperature and feeding history of the copepod (Kiørboe et al., 1982). Two important mechanisms that control the copepods feeding rate are prey concentration and prey size (e.g O'Connors et al., 1980; Jakobsen, 2005; Kiørboe, 2008a; Isari and Saiz, 2011). The effect of prey concentration on the feeding rate is also referred to as the *functional response*. In this study the functional response of the copepod *T. longicornis* was

investigated in relation to prey size. Research on the copepods feeding performance in terms of ingestion and clearance rate provided an opportunity to compare copepod species regarding carbon uptake such as done by Isari and Saiz (2011).

1.2.1 The effect of prey concentration on copepod feeding: the functional response

The feeding rate of a species is dependent on prey availability and a maximum feeding rate is often found at a specific prey concentration (Kiørboe, 2008a). The functional response describes the ingestion of preys by individual predators as a function of prey concentration and is one of the most important behavioral characteristics of predator-prey interactions. The basis of a functional response is that a predator consumes more prey as the density of prey increases (Holling, 1959; Smith and Smith, 2003). The functional response thus relates the per capita predation to prey concentration, but it can also be expressed as proportion of prey ingested per capita per time unit, or *clearance rate* when studying zooplankton. Holling (1959) classifies the functional response into three types, called Holling's type I, II and III.

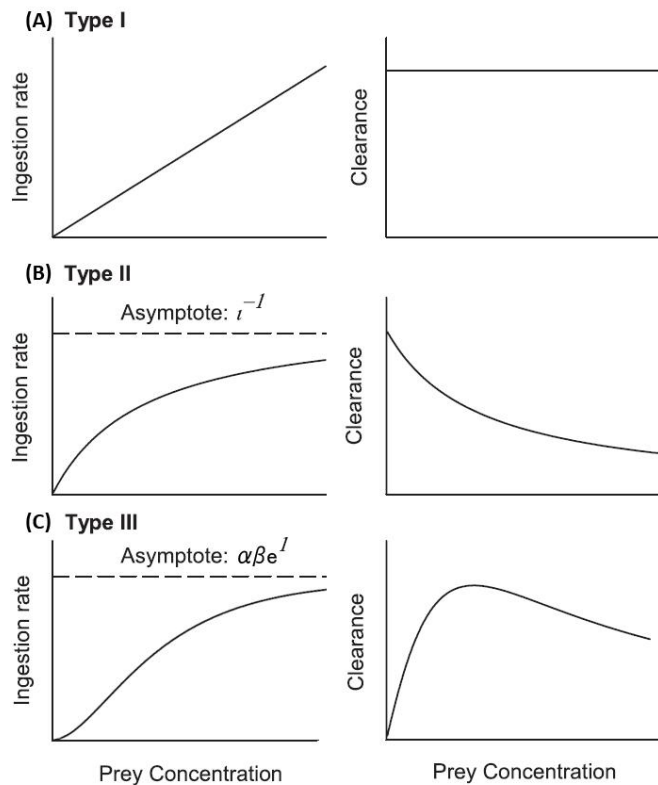


Fig. 3. Three types of functional response curves and expressed as ingestion rate and clearance rate as a function of prey concentration (after Kiørboe, 2008. Asymptote at the type III response is from Schultz and Kiørboe, 2009).

The first type of response (Fig. 3A) describes a linear relation between prey concentration and the ingestion rate and is characteristic for animals that consume food at a rate proportional to their encounter rate of food items (Real, 1977). It implies that the clearance rate of the prey is density independent and thus constant (Smith and Smith, 2003; Kiørboe, 2008a). However, a type I response is not realistically achievable in the long term because a predator needs a certain amount of time to capture and handle their prey (Kiørboe, 2008a). Thus at a certain prey concentration a maximum ingestion rate is reached. This is kind of response is observed for *T. longicornis* by e.g. O'Connors et al. (1980) and Schultz and Kiørboe (2009) and is described by the type II response. The type II functional response (Fig. 3B) describes an ingestion rate that increases in a decelerating fashion with increasing prey density until a saturation level is reached and implies a declining clearance rate with increasing prey concentration (Smith and Smith, 2003). The main factor that causes the ingestion rate to reach a maximum at high prey concentrations is the *handling time*. As the predator catches more prey, the time that it spends handling, eating and digesting the prey results in less time for searching and catching additional prey (Smith and Smith, 2003; Kiørboe, 2008a). The type II functional response can be mathematically described by the disk equation of Holling (Kiørboe, 2008a):

$$I = (\beta C_{prey}) / (1 + \beta \iota C_{prey}) \quad (1.)$$

Where I is the ingestion rate, β is the encounter rate kernel and equals the maximum clearance rate, C_{prey} the concentration of prey and ι the handling time to handle each prey. This formula reveals that at low prey concentrations the ingestion rate is limited by the prey encounter rate and the ingestion rate tends toward the prey encounter rate βC_{prey} . At high prey concentrations the handling time limits the ingestion rate and the ingestion rate tends toward the inverse of the handling time ι^{-1} as depicted in Fig. 3B. The capability of the copepod to reach saturation can be computed by the half saturation constant $C_{\max/2}$ which is equal to $(\beta \iota)^{-1}$ (e.g. Frost, 1972; Isari and Saiz, 2011).

The type III functional response (Fig. 3C) has a potential regulating effect on the prey population. It describes a low ingestion rate at first, then it creases in a sigmoid fashion reaching an equilibrium at high prey density. Plotted as the clearance rate as function of the prey density, the clearance rate is low at a low prey density, rising to a maximum and then decreases. One explanation could be that the predator may switch to other kinds of prey or food source if prey are scarce (Smith and Smith, 2003; Kiørboe, 2008a). A more likely response of the copepod feeding on a monoalgal diet is that the feeding current is reduced or ceases at low prey concentrations, which is observed for several copepods (Kiørboe, 2008a). Van Duren (2000) described that at very low and very high prey concentrations *T. longicornis* shows a relative low swimming speed and at intermediate prey concentrations increased its swimming speed. Swimming speed and the filtering rate are considered to be directly related (Van Duren, 2000), thus this suggests a reduced feeding current at low prey concentrations. The equation describing the sigmoid functional response in ingestion rate as a function of prey concentration is described by Schultz and Kiørboe (2009):

$$I = \alpha \beta e^{1 - \alpha / C_{prey}} \quad (2.)$$

Where I is the concentration-dependent ingestion rate, β is the maximum clearance rate, α the prey concentration where clearance rate is maximum and C_{prey} the prey concentration. The maximum ingestion rate is estimated by $\alpha * \beta * e^1$.

1.2.2 The effect of prey size on copepod feeding: prey size spectrum

Another important factor that determines the feeding rate is prey size. Planktonic predators have an optimal prey size at which their clearance rate is highest (Hansen et al., 1994). This optimal prey-to-predator size ratio is for planktonic predators around 1:10 and for copepods around 1:18 (Hansen et al., 1994). This size-dependant clearance rate can be explained by an increase in prey encounter rate (βC_{prey}) due to a higher percentage of individual cell detections with increasing prey size (Isari and Saiz, 2011). However, preys larger than a certain size are more difficult to handle or could escape more easily which results in an decline in prey capture efficiency (Kiørboe, 2008a). This results in a typical dome-shaped prey size spectrum as shown by Hansen et al. (1994) (Fig. 4).

When the prey size spectrum of *T. longicornis* is known, one could determine the potential prey species and potential clearance rate of this species by its size. *T. longicornis* is able to feed on small prey species such as the algae *Rhodomonas salina* (~6 µm), but is also able to feed on prey that are too large to ingest, such as the *Cosconidiscus wailiesii* (380 µm) by biting a small piece out of the silica cell wall and ingest the cell content only (Jansen, 2008). However,

research on prey size spectrum of *T. longicornis* is scarce and often not the primary goal of the research. A wide range of prey sizes is usually not investigated as monoalgal diets offered in

feeding experiments. However, some experiments are performed using mixed diets. Gentsch et al. (2009) and O'Connors et al. (1980) revealed strong selection by *T. longicornis* for the larger prey in their tested prey range of respectively >12.5 µm ESD (equivalent spherical diameter) and 30.9 µm ESD, consisting of mainly dinoflagellates. Hansen (1995) found a preference for colonies of >100 µm ESD above single cells. In order to determine minimum and maximum feeding rates of *T. longicornis* and their optimal prey-to-predator size ratio, the feeding performance for a wide range of prey sizes needs to be determined.

The effect of prey concentration on the ingestion and clearance rate of *T. longicornis* is examined in several studies at different concentrations and for different prey species (e.g. O'Connors et al., 1980; Klein Breteler et al., 1990; Jakobsen, 2005; Schultz and Kiørboe, 2009). In literature the highest estimated ingestion rates for *T. longicornis* under laboratory tested conditions in terms of carbon consumption were found by Klein Breteler et al. (1990). They found an ingestion rate of $9.1 \cdot 10^6$ pg C copepod⁻¹ day⁻¹ when feeding on the dinoflagellate *Oxyhris marina* (cell size 18 µm ESD, Hansen et al., 1996). The highest estimated clearance rates for *T. longicornis* were found by Shultz and Kiørboe (2009). They found a clearance rate of 51.2 mL copepod⁻¹ day⁻¹ when feeding on *Gyrodinium instriatum* (cell size 31.2 µm ESD, Berge et al., 2008).

However, no studies tested the copepods feeding performance over a larger prey size spectrum including their optimal prey-to-predator size ratio. Thus higher clearance and ingestion rates than found in literature could be expected.

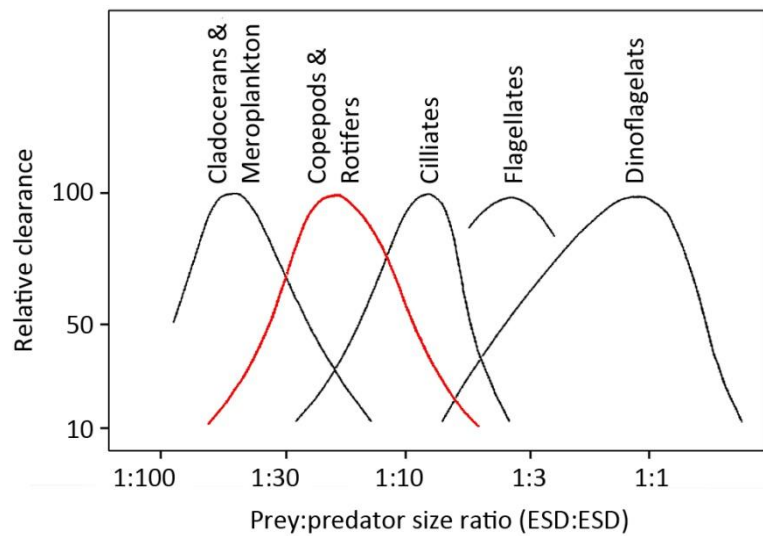


Fig 4. Prey size spectra for individual groups of zooplankton predators expressed as relative clearance vs prey-to-predator size ratio. The red dome-shaped curve shows the prey size spectrum for copepods with an optimal prey-to-predator size ratio of 1:18 (± 3) (after Hansen et al., 1994 and Kiørboe, 2008a).

2. PROBLEM DEFINITION AND AIM

There is a need to understand and quantify the role of zooplankton in large scale biochemical cycles. The feeding response of zooplankton on primary production is a fundamental parameter in ecosystem models and the ocean carbon cycle. Although *T. longicornis* is one of the most abundant copepod species in temperate saline waters of the northern hemisphere, data on functional response and prey size spectrum of the copepod *T. longicornis* is scarce.

While several studies are performed in determining the functional response of *T. longicornis* for specific prey species, or mixtures of prey species, no fundamental experimental research has been conducted dealing with the feeding performance of this species at a wide range of prey sizes of monoalgal diets in order to determine the effect of prey size on the functional response. The aim of this study was to contribute to our current knowledge on calanoid copepod feeding and to provide a basis for future investigation of the zooplankton's distribution and contribution to the carbon cycle by determining the copepod's feeding performance at different concentrations for different sized prey.

In this study the effect of prey concentration on the ingestion and clearance rate is experimentally tested and a functional response model is fitted to the observations. The effect of prey size on the feeding performance of *T. longicornis* is investigated by model estimations of the maximum ingestion and clearance rates for different prey sizes.

The performance of *T. longicornis* in the marine biotic carbon pathway as grazer of the oceans primary production is compared to other copepods by considering maximum ingestion and clearance rates of *T. longicornis* and those of other marine copepods from literature.

3. RESEARCH QUESTIONS

1. Can we explain the ingestion and clearance rate of *T. longicornis* with prey concentration?
 - a. Is the ingestion and clearance rate of *T. longicornis* prey density dependant?
 - b. Which of the functional response models (type II or type III) describes best the effect of prey concentration on the feeding rates of the *T. longicornis*?
2. Are the maximum ingestion and clearance rates of *T. longicornis* dependent on prey size?
 - a. Does prey size affect the estimations of maximum ingestion and clearance rate of *T. longicornis*?
 - b. If there is a relation between prey size and the estimation of the maximum ingestion and clearance rate of *T. longicornis* is there a maximum of the estimation of these rates?
 - c. If there is maximum at what prey size is this maximum of the estimated maximum ingestion and clearance rate reached?
3. Are the estimated maximum ingestion and clearance rates of *T. longicornis* comparable to model estimations of the maximum ingestion and clearance rates of other marine copepods?

4. HYPOTHESIS

- 1a. The ingestion and clearance rate of *T. longicornis* is prey density dependent. Increasing the prey concentration affects the copepods ingestion rate and clearance rate as seen with other calanoid copepods (type II or type III) (e.g. Frost, 1972; Kiørboe, 2008a).
- 1b. Assuming that the feeding current is reduced at low prey concentrations as suggested by Van Duren (2000), the feeding response of *T. longicornis* is best described by a type III functional response.
- 2a. The maximum clearance rate of *T. longicornis* is prey size dependant. Assuming a higher percentage of individual cell detections with increasing prey size, the prey encounter rate will initially increase (e.g. Isari and Saiz, 2011) and then decreases at a certain prey size assuming prey capture efficiency decreases (Kiørboe, 2008a).
- 2b. The model estimated maximum ingestion and clearance rate of *T. longicornis* are expected to be higher than currently described in literature (maximum ingestion rate of $9.1 \cdot 10^6$ pg C copepod⁻¹ day⁻¹, Klein Breteler et al.(1990) and maximum clearance rate of 51.2 mL copepod⁻¹ day⁻¹, Shultz and Kiørboe (2009)), because the feeding rate of *T. longicornis* has not yet be examined over the whole prey size spectrum and the theoretical optimal prey-to-predator size ratio.
- 2c. The maximum clearance rate of *T. longicornis* is prey size-dependent and will be highest at a prey-to-predator size ratio of 1:18 (Hansen et al., 1994).
- 2d. The capability of *T. longicornis* to approach the estimated maximum ingestion rate is inversely dependent on prey size (Frost, 1972; Isari and Saiz, 2011). The copepod will reach satiation at lower prey concentrations with increasing prey size.

5. METHODS

5.1 Experimental design

The functional response of the copepod *T. longicornis* was determined from bottle incubation experiments. The ingestion and clearance rates, expressed as a function of prey concentration, were calculated from the disappearance of food particles in 625 mL incubation bottles containing copepods compared to control bottles without copepods (e.g. Frost, 1972; Uye, 1986; Koski et al., 2005; Isari and Saiz, 2011). The ingestion and clearance rates were studied on 11 monoalgal diets of prey cultures of algae, diatoms or dinoflagellates (Table 2.) varying in size from 6.1 to 58.5 μm (ESD). The dinoflagellate *A. sanguinea* was available in two different cell sizes (33.1 and 42.4 μm ESD) and therefore tested in two separate experiments.

Prey cultures were grown in 0.2 μm filtered sea water (FSW) with a salinity of 32 ‰ with 1.1 mL B1 medium per liter (silicon was added for diatoms). The heterotrophic dinoflagellate *O. marina* was fed on the red algae *R. salina*. Feeding of *O. marina* was stopped four days prior to the experiment to prevent occurrence of *R. salina* in the culture during the experiment. All prey cultures were stock cultures available at the Danish Technical University (DTU Aqua); *C. radiatus* (SCCAP K-1649) was obtained from the Scandinavian Culture Collection of Algae at the University of Copenhagen (SCCAP).

The copepod culture was fed with a mixture of *R. salina*, *T. weissflogii* and *H. triquetra*. Adult females were sorted using a large-mouth pipette under a dissection microscope and starved overnight prior to the start of the experiment. The copepods used in the experiments consisted of cultivated copepods at the DTU and copepods collected in the Øresund strait, approximate 1 km from the coast of Helsingør, Denmark (56°04'N, 12°63'E; ca. 25 m depth at March 22nd and copepods collected between the Skagerrak and Gullmarsfjorden, approximate 500 m from the coast of Kristineberg, Sweden (58°25'N, 11°45'E; ca. 25 m depth) on March 25, 2013. After being selected from the live sample the copepods were gradually let to adjust to experimental temperature of 14 °C. The copepod culture was maintained in the dark at 14 °C.

Each prey species was tested at six different concentrations, based on prey carbon content. Food suspensions were prepared in 0.2 μm FSW (32 ‰ salinity). The average carbon content of the stock cultures was estimated from measurement of the prey concentration (cells mL⁻¹ and μm^3 mL⁻¹) using a Beckman Coulter Multisizer III Coulter Counter (e.g. Isari and Saiz, 2011; Uye, 1986; Frost, 1972) and cell-volume vs carbon content relationship equations described by Menden-Deuer and Lessard (2000), except for *R. salina*. Cell carbon content of *R. salina* was based on measurements by Veloza et al. (2006). To reach the desired concentration, the food suspensions were adjusted through successive dilution. Before incubation, all food suspensions were enriched with 0.4 mL of B1 medium per liter to avoid a difference in algal growth among treatments with copepods and control bottles due to nutrient excretion of the copepods (Isari and Saiz, 2011).

Each experiment consisted of a monoalgal food source, tested at six consecutively doubled concentrations. Six replicate bottles were prepared for each concentration by filling them with 625 mL of suspension. Adult female copepods were added to three of the bottles (the number of copepods was dependent on the food concentration and varied per experiment, but overall 5-12 individuals were used per bottle); these are referred to as “experimental bottles”. Three bottles served as controls (from now on “control bottles”) and a 75 mL sample was taken to record the initial prey concentration. Thereby a sample from each bottle (15 mL or more if less than 400 cells were present in the 15 mL sample) was preserved with 2% Lugol solution for cell counting. After addition of the copepods, the bottles were filled to the top with the corresponding suspension and sealed at the mouth by a screw-cap with a teflon top (i.e. no bubbles inside the bottle). The experimental and

control bottles where mounted on a rotating plankton wheel (0.2 rpm) and incubated for 24 h at 14 °C in the dark. At termination of the experiment, the copepods were carefully filtered out from the sample by pouring the content of each bottle through a 43 µm mesh (or 200 µm mesh for the large dinoflagellate *A. sanguinea* and the large diatom *C. radiatus*) and counted under an inverted microscope (Leica DMIL). Water samples were taken and the cell concentration (cells mL⁻¹ and µm³ mL⁻¹) was determined.

Table 2. Overview of the experiments. The copepods feeding performance was tested for 11 different sized prey at six different concentrations.

Prey species						Copepods		
Species	Description	Size in ESD	Average	Average	Conversion equation	Prosome	Average body	Size in ESD
		(µm)	cell volume	Carbon content	from volume (µm ³) to	length	carbon content	(µm)
			(µm ³)	(pg C cell ⁻¹)	carbon (log pg C cell ⁻¹)	(µm)	(µg cop ⁻¹)	(µm)
<i>Rhodomonas salina</i>	autotrophic red algae/flagellate	6.1 ± 0.4	122	29.8	-	717 ± 32	5.2	475
<i>Thalassiosira weissflogii</i>	diatom < 3000 µm ³	8.6 ± 0.9	362	34.2	-0.541 + 0.811 * log V	850 ± 20	8.8	562
<i>Prorocentrum minimum</i>	mixotrophic thecate dinoflagellate	10.3 ± 0.8	604	199.3	0.175+0.764 * log V	918 ± 16	11.1	608
<i>Oxyhris marina</i>	heterotrophic athecate dinoflagellate	11.4 ± 1.1	868	167.7	-0.05+0.774 * log V	862 ± 17	9.2	571
<i>Heterocapsa triquetra</i>	mixotrophic thecate dinoflagellate	11.9 ± 0.7	883	266.4	0.175+0.764 * log V	955 ± 27	12.5	632
<i>Scripsiella trochoidea</i>	mixotrophic thecate dinoflagellate	15.8 ± 0.9	2157	527.3	0.175+0.764 * log V	859 ± 23	9.0	568
<i>Protoceratium reticulatum</i>	heterotrophic thecate dinoflagellate	22.8 ± 1.7	6538	1230.2	0.175+0.764 * log V	830 ± 18	8.2	550
<i>Lingulodinium polyedrum</i>	mixotrophic thecate dinoflagellate	23.8 ± 1.2	7367	1347.8	0.175+0.764 * log V	908 ± 27	10.7	601
<i>Akashiwo sanguinea</i>	mixotrophic athecate dinoflagellate	33.1 ± 1.6	19622	1873.2	-0.05+0.774 * log V	904 ± 21	10.6	598
<i>Akashiwo sanguinea</i>	mixotrophic athecate dinoflagellate	42.4 ± 2.9	41646	3353.9	-0.05+0.774 * log V	798 ± 22	7.2	528
<i>Coscinodiscus radiatus</i>	diatom > 3000 µm ³	58.5 ± 6.3	106829	3142.5	-0.933 + 0.881 * log V	790 ± 11	7.0	523

Prey size (in ESD) and average cell volume was estimated with a Beckman Coulter Multisizer III. Carbon content per cell is estimated from average cell volume and volume to carbon conversion equations described by Menden-Deuer and Lessard (2000). For dinoflagellates a distinction was made between ‘thecate’ and ‘athecate’ species for assigning the conversion equation. Cell carbon content for *R. salina* is as determined by Veloza et al. (2006). Copepod prosome length was measured for at least 10 randomly chosen copepods after termination of the experiment. Copepod carbon content was estimated by converting average prosome length to ash free fry weight as described by Klein Breteler et al. (1982) and assuming a carbon content of 46% of the ash free dry weight (Nielsen and Andersen, 2002). Copepod ESD was calculated from volume according to Hansen et al. (1994) and copepod volume from the length to volume equation described in Jiang and Kiorboe (2011), assuming the copepod has a prolate spheroid shape with an aspect ratio of 0,54 (aspect ratio calculated from measurements of *T. longicornis* in Conway (2006)).

5.2 Data analysis

5.2.1 Calculation of prey concentration, clearance and ingestion rates

The ingestion and clearance rates and the average prey concentration during the experiment were calculated for each concentration according to the simplified equations of Frost (1972) as described in Kjørboe et al. (1982). The growth constant *k* for prey growth during the incubation period is calculated with the following equation

$$C_2 = C_1 e^{k(t_2 - t_1)} \quad (3.)$$

were C_1 and C_2 are the prey concentration in the control bottle at respectively t_1 and t_2 . For each experimental bottle the grazing coefficient, *g*, is defined as

$$C_2^* = C_1^* e^{(k-g)(t_2 - t_1)} \quad (4.)$$

where C_1^* and C_2^* are the cell concentrations in the experimental bottles at the beginning (t_1) and the end (t_2) of the experiment. The average prey concentration [*C*] in each experimental bottle during incubation period is calculated as

$$[C] = (C_1^* e^{(k-g)(t_2 - t_1)} - C_1^*) / ((t_2 - t_1)(k - g)) \quad (5.)$$

The clearance rate was calculated by multiplying the volume of the bottle and the grazing coefficient, and then dividing it by the number of living copepods N in the bottle:

$$F = Vg/N \quad (\text{mL cop}^{-1} \text{ day}^{-1}) \quad (6.)$$

Frost's equations were simplified as described in Kiørboe et al. (1982) by isolating k and g from equation (3.) and (4.) and substituting in equations (5.) and (6.). Equation (5.) simplifies to

$$[C] = (C_2^* - C_1^*)/\ln(C_2^*/C_1^*) \quad (\mu\text{g C mL}^{-1}) \quad (7)$$

And equation (6.) to

$$F = (V/Nt)\ln((C_1^* - C_2)/(C_1 - C_2^*)) \quad (\text{mL cop}^{-1} \text{ day}^{-1}) \quad (8.)$$

where $t = t_2 - t_1$. The ingestion rate, I , can be calculated by multiplying the clearance rate by the average prey concentration during the incubation period:

$$I = F*[C] \quad (\mu\text{g C cop}^{-1} \text{ day}^{-1}) \quad (9.)$$

The clearance and ingestion rates were calculated according to respectively equation 8 and 9. The difference in prey concentration between control bottles and experimental bottles were compared with a Student's t-test using the software SPSS statistics 20. The effect of prey concentration on the feeding rate of the *T. longicornis* is illustrated by plotting the clearance and ingestion rates against the average prey concentration for all prey sizes. The data was expressed prey carbon basis ($\mu\text{g C mL}^{-1}$), making comparison between other species and results in many other studies possible (e.g. Weiße, 1983; Klein Breteler and Koski, 2003; Koski et al., 2005).

Since copepod size varied between experiments, in order to make it possible to compare copepod feeding performance of all experiments, carbon-specific ingestion rates for each prey species were also estimated taking into account the average copepod biomass (carbon) in each experiment. Copepod biomass (ash-free dry weight) was estimated using the prosome length-biomass relation for cultured *T. longicornis* copepodites according to Klein Breteler et al. (1982) and carbon content was calculated assuming a carbon content of 46% of the ash-free dry weight (Nielsen and Andersen, 2002). The average copepod length in each experiment was estimated by measuring the prosome length of at least 10 randomly chosen individuals immediately after termination of the incubation under an inverted microscope (Leica DMIL) with an ocular micrometer.

5.2.2 Fitting the functional response model

To assess the dependence of the clearance and ingestion rates on prey concentration a functional response model (Holling type II and III) was fitted to the observations using the software SigmaPlot 12.0. The software calculates the model parameters which minimize the sum of squared difference between the values of the measured and predicted values of the clearance and ingestion rate. By fitting the model to the observations, values of maximum clearance rate, prey handling time and maximum ingestion rate were estimated (Kiørboe, 2008a; Shultz and Kiørboe, 2009). A Hollings type II model was fitted to the measured ingestion rates and carbon specific ingestion rates:

$$I = (\beta C_{prey})/(1+\beta\iota C_{prey}) \quad (\mu\text{g C cop}^{-1} \text{ day}^{-1}) \quad (1.)$$

where β is the maximum clearance rate (mL day^{-1}), ι prey handling time (day) and ι^{-1} the maximum ingestion rate ($\mu\text{g C mL}^{-1}$). The capability of the copepod to approach saturation is computed by the

half saturation constant, $C_{lmax/2}$ and is calculated as $(\beta I)^{-1}$. This constant represents the concentration at which the ingestion rate equals half of the maximum ingestion rate I_{max} . Thereby the model describing a Holling type III functional response was fitted to the data (Shultz and Kiørboe, 2009; Kiørboe et al., 1982):

$$I = \alpha \beta e^{1-\alpha/C_{prey}} \quad (\mu\text{g C cop}^{-1} \text{ day}^{-1}) \quad (2.)$$

where $\alpha \beta e^1$ equals the maximum ingestion rate and α the prey concentration at which clearance rate is maximum (Schultz and Kiørboe, 2009). Prey handling time was not estimated with the equation describing a Holling type III functional response, since the equation does not include this parameter. The statistical fit of the type II and III regressions to the data was compared by the coefficient of determination.

To assess the dependence of the clearance rate on prey size, the estimated maximum clearance rates (from fitting the Holling type II and III model) of all experiments were plotted as function of prey to predator size ratio (in ESD:ESD) (e.g. Hansen et al., 1994; Kiørboe, 2008a). To assess the dependence of the ingestion rate on prey size, the estimated maximum carbon specific ingestion rates (from fitting the Holling type II and III model) and half saturation constant (from fitting the Holling type II model) of all experiments were plotted as function of prey size (in ESD) (e.g. Isari and Saiz, 2011).

To estimate copepod size in ESD the copepods volume was calculated from the length to volume equation described in Jiang and Kiørboe (2011), assuming the copepod has prolate spheroid shape

$$V_{copepod} = 4/3\pi\eta^2 a^3 \quad (\mu\text{m}^3) \quad (10.)$$

where a is half the prosome length and η the aspect ratio, assuming the shape of a prolate spheroid with the major axis equals prosome length and the minor axes equals $\eta \times$ prosome length. The copepod aspect ratio η was calculated from length and prosome width measurements of adult female *T. longicornis* described in Conway (2006). Copepod volume was converted to ESD according to Hansen et al. (1994) by

$$ESD = (volume/0,523)^{1/3}. \quad (\mu\text{m}) \quad (11.)$$

5.2.3 Comparative analysis

To compare *T. longicornis* to other copepods as grazers of phytoplankton, results of the bottle incubations were compared to the feeding performance of other marine copepods from literature.

Therefore log-transformed maximum clearance rates and ingestion rates were plotted as function of log transformed copepod size (ESD in μm). The maximum clearance and ingestion rate of the *T. longicornis* were compared to the linear regression fitted to rates for all marine copepods from literature. A dataset of feeding rates on single prey of other marine copepods assembled by Kiørboe (unpublished data) was used. Only data for copepods in naupli and copepodite stage feeding on single prey, smaller than its predator (prey might be ingested only partially) were used. In the mentioned database, experiments were conducted at different temperatures, therefore all rates were corrected for temperature to the experimental temperature of the current study (14 °C) with a temperature dependence coefficient Q_{10} of 2,8 (as in Kiørboe, unpublished data). Copepod size was estimated by converting copepod carbon content to copepod volume using the conversion regression described in Hansen et al. (1994), where carbon was converted to volume by a factor of $8.3 \mu\text{m}^3 \text{ pg C}^{-1}$. Copepod ESD was then calculated from volume with equation 11. The maximum

ingestion and clearance rates were determined using different techniques (e.g. particle removal, gut pigment technique) and different models were fitted to the data to determine maximum ingestion and clearance rates.

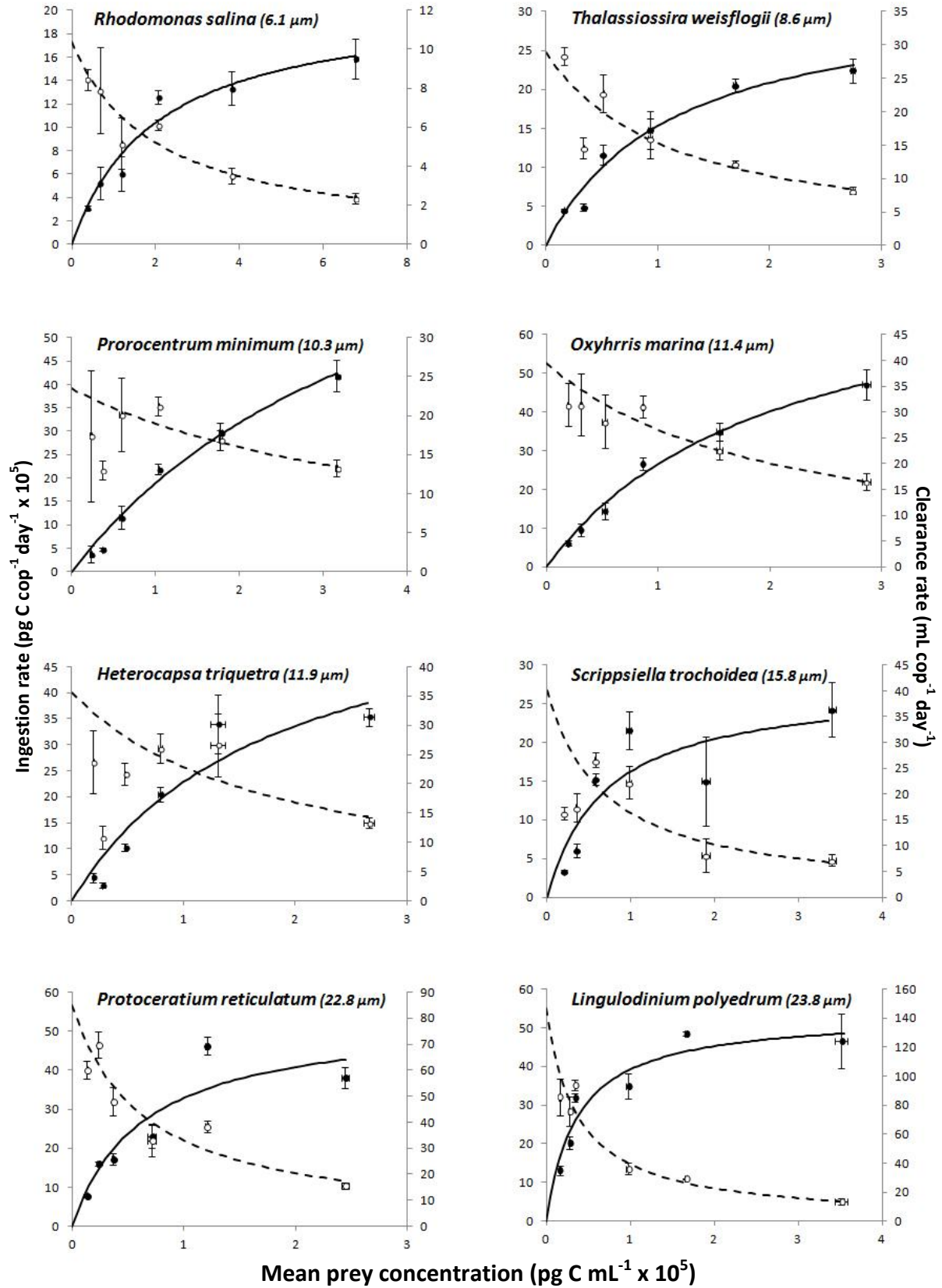
6. RESULTS

6.1 The effect of prey concentration on the ingestion and clearance rate

T. longicornis ingested all prey species at a concentration-dependant rate. The ingestion rate increased with prey concentration and showed in all cases a tendency towards an asymptotic maximum. The clearance rate declined in all experiments with increasing prey carbon concentration as shown in Fig. 5 and Fig. 6. Appendix I shows all measured ingestion and clearance rates and the significance of ingestion of prey (in number of prey cells) in the experimental bottles compared to the control bottles for all tested prey species.

To determine what functional response model described the observations best a Holling type II and Holling type III functional response equation were fitted to the measured ingestion rates for 11 different sizes of prey. Fitting the Holling type III equation to the observations showed a more conservative estimation of model parameters than when a Holling type II equation was fitted. Due to difference in model parameters and estimation of similar model parameters between the type II and type III equation, a comparison between prey species is made for the separate model fits. The assemblage of results for the type II fit is compared to the assemblage of results of the type III fit.

For several prey species the observations implied a typical type III response and for other prey the observations implied a type II shaped response. Fitting both models to the observations showed only small differences in the coefficient of determination, as shown in Table 3 and Table 4. Fitting the Holling type II model to the observations gave an average coefficient of determination of 0.730 and showed a better fit to the observations of ingestion rate of the prey species *R. salina*, *T. weisflogii*, *O. marina*, *P. reticulatum*, *C. radiatus*. When a Holling type III model was fitted the average coefficient of determination was 0.738 and showed a better fit to the observations of ingestion rate of the prey species *P. minimum*, *H. triquetra*, *S. trochoidea*, *L. polyedrum*, *A. sanguinea*. The functional response of *T. longicornis* is presented in Fig. 5 with a Holling type II fitted model and in Fig. 6 with a Holling type III fitted model.



Mean prey concentration (pg C mL⁻¹ x 10⁵)

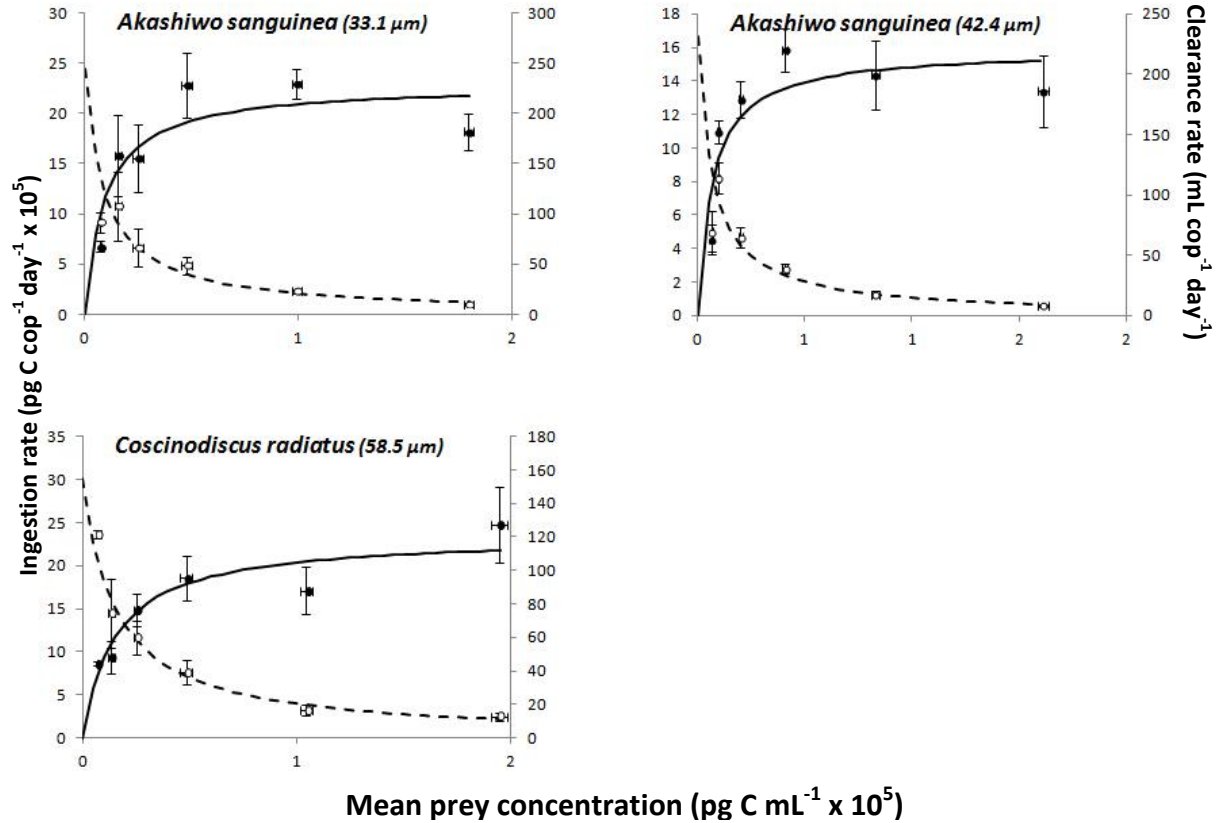
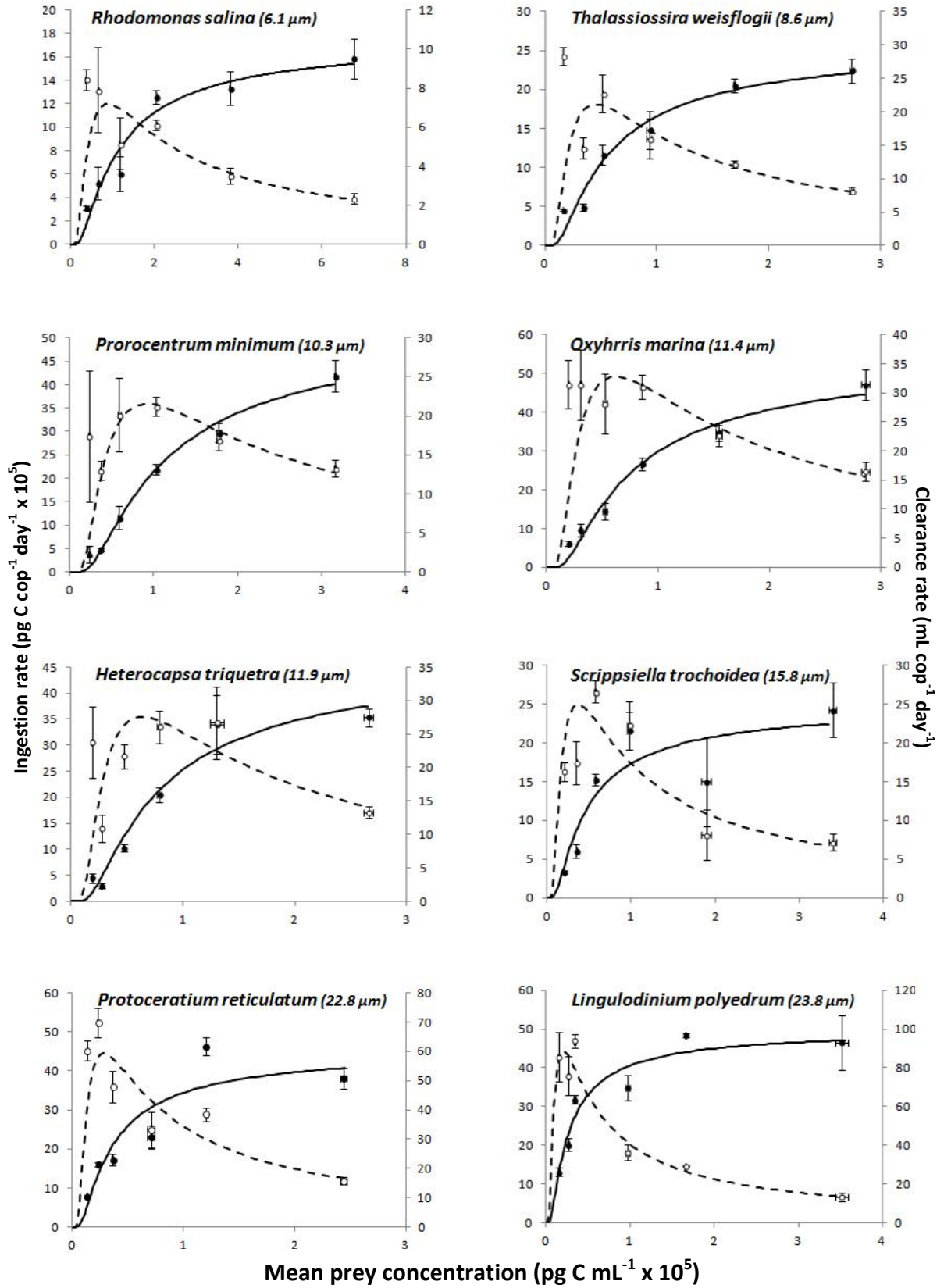


Fig. 5. Functional response of *T. longicornis* on different prey sizes. Ingestion (pg C cop⁻¹ day⁻¹) and clearance rates (mL cop⁻¹ day⁻¹) are presented as function of the average prey concentration (pg C mL⁻¹) during the experiment. Closed circles represent the average measured ingestion rate of three replicates and open circles the clearance rate. The vertical and horizontal error bars indicate one standard error of the mean value of three replicates. Solid lines are fits of Holling type II functional response curve equation 1 to the measurements for ingestion rate and dotted lines of clearance rate via equation 9. Estimates of parameters of the fitted model are given in Table 3. Note the different scales in X and Y axis for each panel.

Table 3. Parameter and standard error estimates for functional response curve fits for ingestion rate expressed in carbon (pg C cop⁻¹ day⁻¹) and carbon-specific ingestion rate (μg C mg C⁻¹ day⁻¹). Maximum clearance rate (β) and prey handling time (ι) are estimated by Holling type II functional response curve equation 1. Maximum ingestion rate (I_{max}) is the inverse of the handling time and prey concentration at maximum ingestion rate equals the inverse of ι . Indication of the fit to measurements of the Holling type II model is given by the coefficient of determination.

Ingestion rate, Holling type II model fit								
Prey species	Ingestion rate (pg carbon cop ⁻¹ day ⁻¹)				Carbon specific ingestion rate (μg C mg C ⁻¹ day ⁻¹)			
	Maximum ingestion rate, I_{max} (pg C cop ⁻¹ day ⁻¹)	Maximum clearance rate, β (mL day ⁻¹)	Handling time, ι (day)	Prey concentration at max $I/2$, $C_{I_{max}/2}$ (pg C mL ⁻¹)	R^2	Maximum ingestion rate, I_{max} (μg C mg C ⁻¹ day ⁻¹)	Maximum clearance rate, β (mL mg C ⁻¹ day ⁻¹)	
<i>R. salina</i>	2.1E+06 ± 2.9E+05	10.4 ± 2.2	4.8E-07 ± 6.5E-08	2.0E+05 ± 5.1E+04	0.81	402 ± 55	1993 ± 425	
<i>T. weissflogii</i>	3.3E+06 ± 4.1E+05	28.9 ± 4.6	3.1E-07 ± 3.9E-08	1.1E+05 ± 2.3E+04	0.89	372 ± 47	3301 ± 530	
<i>P. minimum</i>	9.9E+06 ± 2.6E+06	23.4 ± 3.1	1.0E-07 ± 2.7E-08	4.2E+05 ± 1.2E+05	0.93	895 ± 236	2113 ± 283	
<i>O. marina</i>	8.2E+06 ± 1.2E+06	39.4 ± 4.9	1.2E-07 ± 1.9E-08	2.1E+05 ± 4.1E+04	0.93	891 ± 136	4301 ± 534	
<i>H. triquetra</i>	6.4E+06 ± 1.7E+06	35.6 ± 8.1	1.6E-07 ± 4.2E-08	1.8E+05 ± 6.3E+04	0.82	508 ± 135	2845 ± 650	
<i>S. trochoidea</i>	2.7E+06 ± 5.7E+05	40.0 ± 15.3	3.6E-07 ± 7.5E-08	6.9E+04 ± 3.0E+04	0.56	304 ± 63	4429 ± 1695	
<i>P. reticulatum</i>	5.4E+06 ± 7.8E+05	85.1 ± 19.4	1.9E-07 ± 2.7E-08	6.3E+04 ± 1.7E+04	0.78	658 ± 96	10430 ± 2374	
<i>L. polyedrum</i>	5.3E+06 ± 4.5E+05	146.9 ± 29.6	1.9E-07 ± 1.6E-08	3.6E+04 ± 7.9E+03	0.79	498 ± 42	13689 ± 2762	
<i>A. sanguinea</i> (33,1 μm)	2.3E+06 ± 2.7E+05	243.9 ± 102.4	4.4E-07 ± 5.1E-08	9.4E+03 ± 4.1E+03	0.44	216 ± 25	23047 ± 9671	
<i>A. sanguinea</i> (42,4 μm)	1.6E+06 ± 1.5E+05	231.8 ± 81.7	6.3E-07 ± 5.9E-08	6.8E+03 ± 2.5E+03	0.51	219 ± 21	32094 ± 11318	
<i>C. radiatus</i>	2.3E+06 ± 2.7E+05	154.6 ± 50.3	4.3E-07 ± 4.9E-08	1.5E+04 ± 5.2E+03	0.57	335 ± 38	22104 ± 7190	



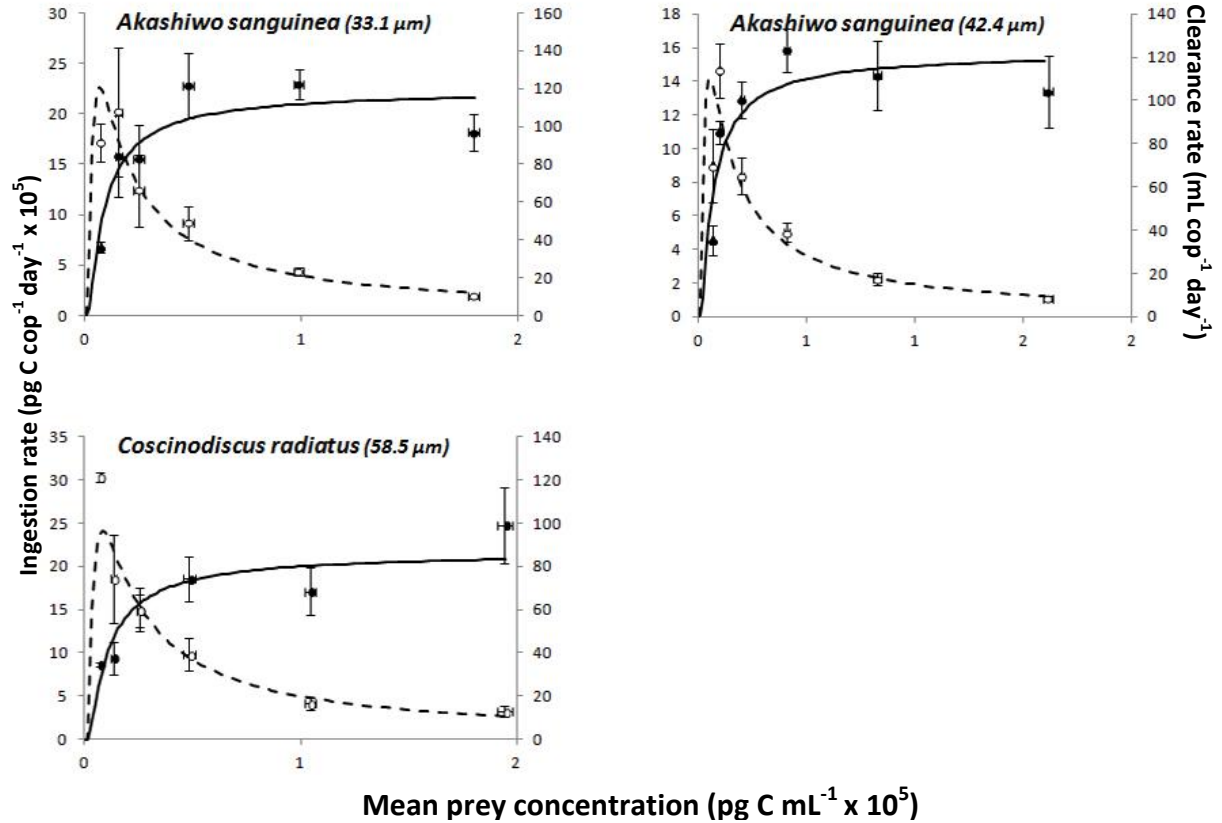


Fig. 6. Functional response of *T. longicornis* on different prey sizes. Ingestion ($\text{pg C cop}^{-1} \text{ day}^{-1}$) and clearance rates ($\text{mL cop}^{-1} \text{ day}^{-1}$) are presented as function of the average prey concentration (pg C mL^{-1}) during the experiment. Closed circles represent the average measured ingestion rate of three replicates and open circles the clearance rate. Horizontal and vertical error bars indicate one standard error of the mean value of three replicates. Solid lines are fits of Holling type III functional response curve equation 2 to the measurements and dotted lines of of clearance rate via equation 9. Estimates of parameters of the fitted model are given in Table 4. Note the different scales in X and Y axis for each panel.

Table 4. Parameter and standard error estimates for functional response curve fits for ingestion rate expressed in carbon ($\text{pg C cop}^{-1} \text{ day}^{-1}$) and carbon-specific ingestion rate ($\mu\text{g C mg C}^{-1} \text{ day}^{-1}$). Maximum clearance rate (β) and concentration at maximum clearance rate (α) are estimated by Holling type III functional response curve equation 2. Maximum ingestion rate (I_{max}) equals $\alpha\beta e^{-1}$. Indication of the fit of the Holling type III model to the observations is given by the coefficient of determination.

Prey species	Ingestion rate, Holling type III model fit				Carbon specific ingestion rate ($\mu\text{g C mg C}^{-1} \text{ day}^{-1}$)	
	Maximum ingestion rate, I_{max} ($\text{pg C cop}^{-1} \text{ day}^{-1}$)	Maximum clearance rate, β (mL day^{-1})	Prey concentration at max clearance rate, α (pg C mL^{-1})	R^2	Maximum ingestion rate, I_{max} ($\mu\text{g C mg C}^{-1} \text{ day}^{-1}$)	Maximum clearance rate, β ($\text{mL mg C}^{-1} \text{ day}^{-1}$)
<i>R. salina</i>	$1.8\text{E}+06 \pm 4.1\text{E}+05$	7.2 ± 1.0	$9.0\text{E}+04 \pm 1.7\text{E}+04$	0.80	338 ± 79	1381 ± 189
<i>T. weissflogii</i>	$2.6\text{E}+06 \pm 4.6\text{E}+05$	21.1 ± 2.1	$4.5\text{E}+04 \pm 6.6\text{E}+03$	0.87	298 ± 53	2410 ± 244
<i>P. minimum</i>	$5.4\text{E}+06 \pm 7.1\text{E}+05$	21.5 ± 1.5	$9.2\text{E}+04 \pm 1.0\text{E}+04$	0.93	485 ± 64	1938 ± 131
<i>O. marina</i>	$5.6\text{E}+06 \pm 7.9\text{E}+05$	32.8 ± 2.5	$6.2\text{E}+04 \pm 7.4\text{E}+03$	0.92	606 ± 86	3582 ± 277
<i>H. triquetra</i>	$4.8\text{E}+06 \pm 9.1\text{E}+05$	27.6 ± 2.8	$6.4\text{E}+04 \pm 1.0\text{E}+04$	0.87	381 ± 72	2202 ± 222
<i>S. trochoidea</i>	$2.5\text{E}+06 \pm 9.3\text{E}+05$	25.0 ± 5.5	$3.7\text{E}+04 \pm 1.1\text{E}+04$	0.60	277 ± 102	2764 ± 610
<i>P. reticulatum</i>	$4.6\text{E}+06 \pm 1.1\text{E}+06$	59.2 ± 8.6	$2.8\text{E}+04 \pm 5.6\text{E}+03$	0.77	560 ± 136	7262 ± 1048
<i>L. polyedrum</i>	$5.0\text{E}+06 \pm 1.0\text{E}+06$	88.7 ± 11.5	$2.1\text{E}+04 \pm 3.3\text{E}+03$	0.79	465 ± 96	8271 ± 1069
<i>A. sanguinea (33,1 μm)</i>	$2.2\text{E}+06 \pm 9.9\text{E}+05$	120.8 ± 34.3	$6.8\text{E}+03 \pm 2.3\text{E}+03$	0.47	212 ± 94	11413 ± 3240
<i>A. sanguinea (42,4 μm)</i>	$1.6\text{E}+06 \pm 5.7\text{E}+05$	110.1 ± 25.7	$5.3\text{E}+03 \pm 1.5\text{E}+03$	0.55	218 ± 79	15243 ± 3560
<i>C. radiatus</i>	$2.2\text{E}+06 \pm 8.1\text{E}+05$	96.8 ± 23.1	$8.3\text{E}+03 \pm 2.4\text{E}+03$	0.54	311 ± 116	13840 ± 3306

6.2 The effect of prey size on the ingestion and clearance rate

6.2.1 The effect of prey size on ingestion rate

The observed maximum ingestion rates varied among prey species and a maximum average ingestion rate of $48.4 \cdot 10^5$ pg C copepod⁻¹ day⁻¹ was observed for the relative large dinoflagellate *L. polyedrum*. The estimated maximum ingestion rates ranged from $1.6 \cdot 10^6$ to $9.9 \cdot 10^6$ pg C copepod⁻¹ day⁻¹ when the Holling type II model was fitted to the observations and showed a lower estimate, from $1.6 \cdot 10^6$ to $5.6 \cdot 10^6$ pg C copepod⁻¹ day⁻¹, when a Holling type III model was fitted.

To determine the effect of prey size on the maximum ingestion rate the model estimations of carbon-specific maximum ingestion rates were plotted in relation to prey size. No clear effect of prey size on the maximum ingestion rate was observed as shown in Fig. 7A. The estimated carbon-specific maximum ingestion rates ranged from 216 to 895 $\mu\text{g C mg C}^{-1} \text{ day}^{-1}$ the Hollings type II model fit and was with 212 to 606 $\mu\text{g C mg C}^{-1} \text{ day}^{-1}$ lower for the Hollings type III fitted model. The highest carbon-specific maximum ingestion rates were found for the relative small *P. minimum* (10.3 μm ESD) with a Hollings type II model fit and the relative small *O. marina* (11.4 μm ESD) with a Hollings type III model fit.

The capability of the copepod to approach saturation for the different sized prey was computed by the half saturation constant, $C_{I_{max}/2}$. The results show as the size of prey increases the carbon concentration at which half the maximum ingestion rate was reached decreased and was lowest for the relative large *Akashiwo sanguinea* (33.1 μm ESD) as shown in Fig. 7B. The estimation of the maximum ingestion rates (I_{max}) and half saturation constant $C_{I_{max}/2}$ and carbon specific maximum ingestion rates are shown in Table 3 (Holling type II fit) and Table 4 (Holling type III fit).

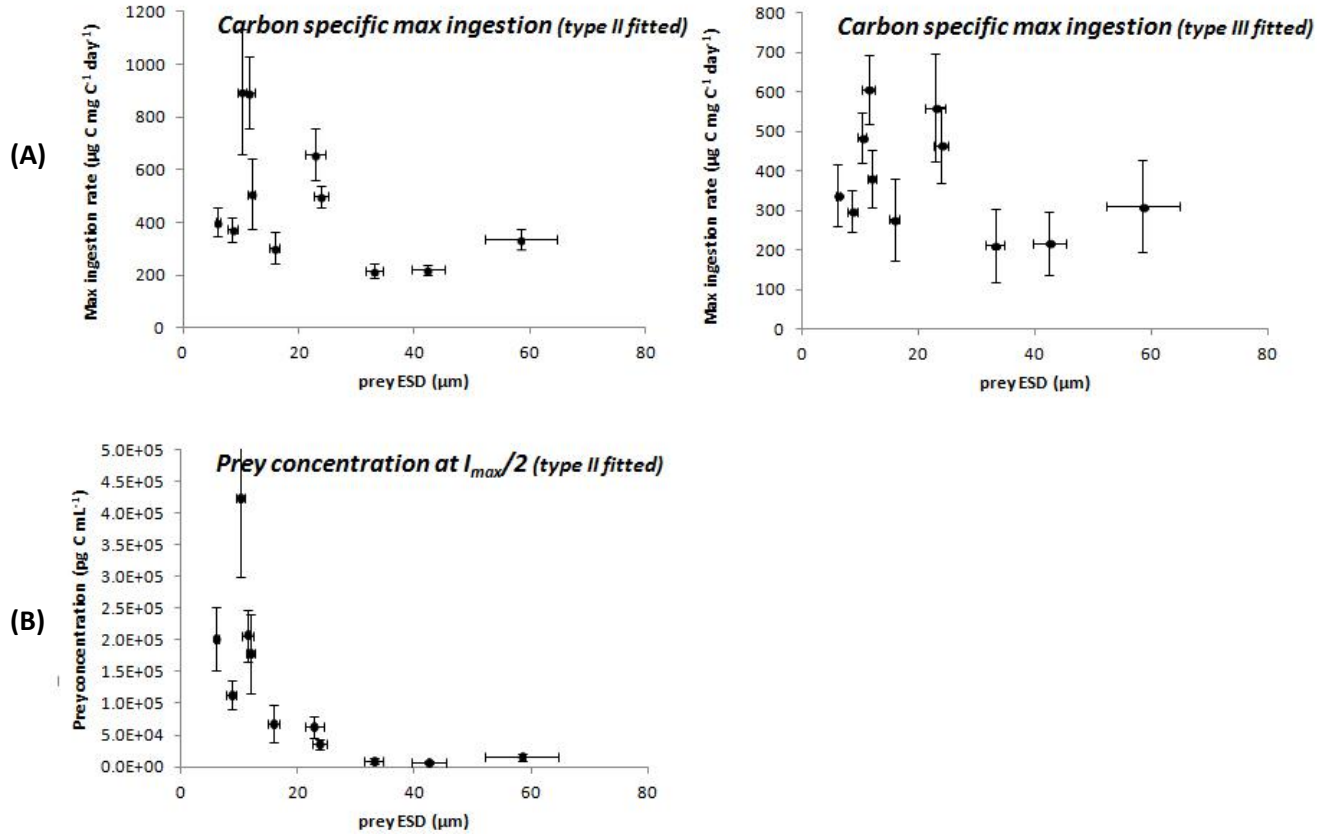


Fig. 7. Model estimations of the maximum ingestion rate expressed in carbon-specific ingestion rate ($\mu\text{g C mg C}^{-1} \text{ day}^{-1}$) (A) and the prey concentration at half the maximum ingestion rate as function of prey size (ESD in μm) (B). The error bars indicate one standard error of the estimated model parameters. Estimates of the model parameters are given in Table 3 (type II model fit) and Table 4 (type III model fit). Note the different scales in Y axis for each panel.

6.2.2 The effect of prey size on clearance rate

The observed maximum clearance rates varied among prey species and a maximum average clearance rate of $113.7 \text{ mL copepod}^{-1} \text{ day}^{-1}$ was observed for the dinoflagellate *Akashiwo sanguinea* ($42.4 \mu\text{m}$ ESD). The estimated maximum clearance rate ranged from $10.4 \text{ mL copepod}^{-1} \text{ day}^{-1}$ for the smallest prey, *Rhodomonas salina* ($6.1 \mu\text{m}$ ESD), up to $243.9 \text{ mL copepod}^{-1} \text{ day}^{-1}$ for the relative large prey *Akashiwo sanguinea* ($33.1 \mu\text{m}$ ESD) when the Holling type II model was fitted. Clearance rates were considerably lower when the Holling type III model was fitted and ranged from $7.2 \text{ mL copepod}^{-1} \text{ day}^{-1}$ (*Rhodomonas salina*) up to $120.8 \text{ mL copepod}^{-1} \text{ day}^{-1}$ (*Akashiwo sanguinea*).

To determine the effect of prey size on the maximum clearance rate the model estimations of the maximum clearance rates were plotted in relation to prey-to-predator size ratio. The maximum clearance rate clearly increased with prey size up to a maximum and then decreased with prey size. The highest clearance rates for *T. longicornis* were found between a prey:predator size ratio of 0.055 and 0.080 as shown in Fig. 8. The estimation of the maximum clearance rate for each prey (β) are shown in Table 3 (Holling type II fit) and Table 4 (Holling type III fit).

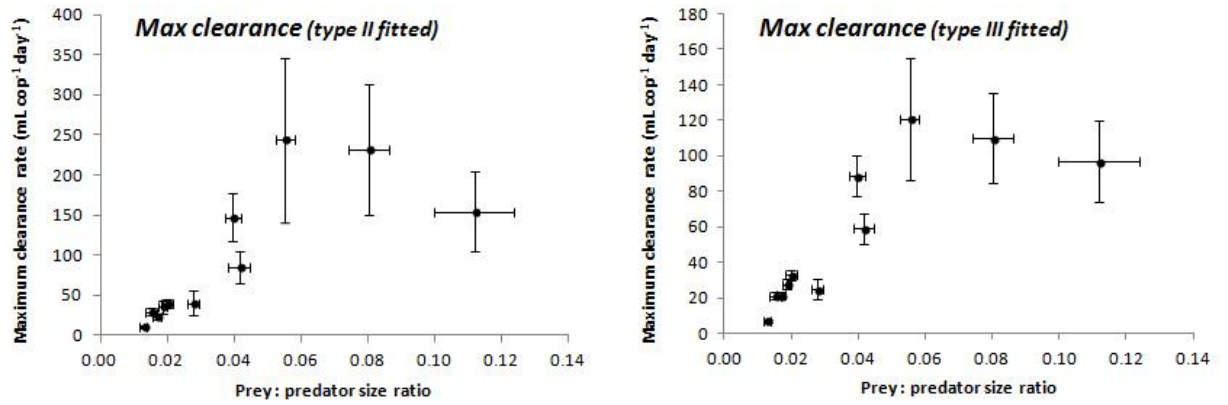


Fig. 8. Model estimations of the maximum clearance rates as function of prey: predator size ratio. The error bars indicate one standard error of the estimated model parameters. Estimates of the model parameters are given in Table 3 (type II model fit) and Table 4 (type III model fit). Note the different scales in Y axis for each panel.

7. DISCUSSION

7.1 The effect of prey concentration on the ingestion and clearance rate

7.1.1 Prey density dependant ingestion and clearance rate

The copepod *T. longicornis* showed for all prey species a typically density dependent ingestion and clearance rate as in other studies on the effect of prey density on feeding of *T. longicornis* (O'Connors, 1980; Vincent and Hartman, 2001; Jakobsen 2005; Schultz and Kiørboe, 2009). The ingestion rate increased with increasing prey concentration up to an maximum and the clearance rate declined in all experiments with increasing prey carbon concentration. The range of prey carbon concentrations in the experiments of smaller prey species (6.1 μm – 22.8 μm ESD) however did not allow full satiation, while in case of larger prey (23.8 μm – 58.5 μm ESD) full satiation was reached. Therefore, the maximum ingestion rates of *T. longicornis* determined by the fitted equations are taken as a proxy for the potential maximum ingestion rate for those species.

7.1.2 Fitting the functional response model

Fitting the observations to both models showed only small differences in statistical fit to the measurements (Table 3 and 4) and thus could not provide evidence for what model best describes the functional response of *T. longicornis*. The functional response in several experiments suggested a potential type III functional response (Fig. 5 and 6), which was most evident for *P. minimum*, *H. triquetra*, *S. throchoidea* and *A. sanguinea* (33.1 and 42.4 μm). This was statistically supported by a better fit for the type III model to the observations of ingestion rate of the prey species *P. minimum*, *H. triquetra*, *S. throchoidea*, *A. sanguinea*. However, also *L. polyedrum* showed a better fit while the observations suggested a typical type II response. Thereby the observations were not conclusive to determine the best model. First of all because the lowest concentration tested might have been not low enough to show a type III feeding response in the observations and thus implies a type II response. Secondly, because there are few observations at the lower range of tested prey concentrations and there is a substantial spread in replicates.

However, a biological explanation shows that a type III response is most convincing. Copepods are able to detect the quality and quantity of food particles through chemo- and mechanoreception and are able to change their feeding mode and the intensity of thier movements according to this information (DeMott and Watson, 1991; Van Duren, 2000). Lehman (1976) predicted that the optimal foraging strategy would be a low filtering rate at low prey concentrations and high concentrations. This is emperically supported by Kiørboe (2008a) and Van Duren (2000). Kiørboe (2008a) described that in several studies the generation of the feeding current ceases or is reduced by copepods when encountering low prey concentrations which could explain the observation of a typical type III functional response. Van Duren (2000) observed a decrease in swimming speed of adult *T. longicornis* females at very low prey concentrations when fed on *R. salina*. If swimming speed is considered to be directly related to the filtering rate, a decreased prey concentration decreases the chance of prey encounter and thus a decreased clearance rate at low prey concentrations. When more prey are present, the feeding current increases and clearance rate increases. At even higher prey concentrations, the clearance starts decreasing because the copepod

can sustain a high capture rate at a reduced generation of feeding current and thus at low energetic costs.

7.2 The effect prey size on the ingestion and clearance rate

7.2.1 The effect of prey size on the ingestion rate

The observed maximum ingestion rates varied strongly among prey species and a maximum average ingestion rate of $48.4 \cdot 10^5$ pg C copepod⁻¹ day⁻¹ was reached for the relative large dinoflagellate *L. polyedrum*. The estimated maximum ingestion rates ranged from $1.6 \cdot 10^6$ to $9.9 \cdot 10^6$ pg C copepod⁻¹ day⁻¹ when the Holling type II model was fitted to the observations and showed a lower estimate, from $1.6 \cdot 10^6$ to $5.6 \cdot 10^6$, when a Holling type III model was fitted. The difference in the estimations of the maximum ingestion rate by the different models could be explained by the fact that the models estimate the maximum ingestion rate for several prey species at prey concentrations much higher than tested in the experiments. The highest ingestion rates were estimated for *P. minimum* and *O. marina*. When looking at the observations of the ingestion rate of these two dinoflagellates and the fitted models in Fig. 5 and 6. the ingestion rate suggest little saturation in the range of the tested prey concentrations. Testing the ingestion rate for higher prey concentrations could give a more robust estimation of the ingestion maxima for both models.

The estimated maximum ingestion rate when the Holling type II model was fitted was comparable to the estimated maximum ingestion rate in earlier studies. The highest estimation for ingestion rate for *T. longicornis* of $9.1 \cdot 10^6$ pg C copepod⁻¹ day⁻¹ was made by Klein Breteler et al. (1990). Different from O'Connors et al. (1980) and Gentsch et al. (2009) the estimated maximum ingestion rate of *T. longicornis* in this study did not increase with prey size (Fig. 7A), but varied for strongly different prey sizes.

The actual carbon ingestion could be overestimated for the large diatom *C. radiatus* in Fig. 7A. The ingestion rate of prey in this research was presented as prey carbon. However, when the maximum ingestion was expressed as ingested prey volume, it occurred that the ingestion of *C. radiatus* was much higher than ingestion of other prey species. This was not observed when looking at ingestion in terms of carbon due to the low carbon concentration of diatoms compared to the dinoflagellates used in this experiment (Fig 9). The observed high carbon ingestion could be explained by 'sloppy feeding' of the copepod as described by Jansen (2008). Jansen observed destruction of the cell wall and partial ingestion of the

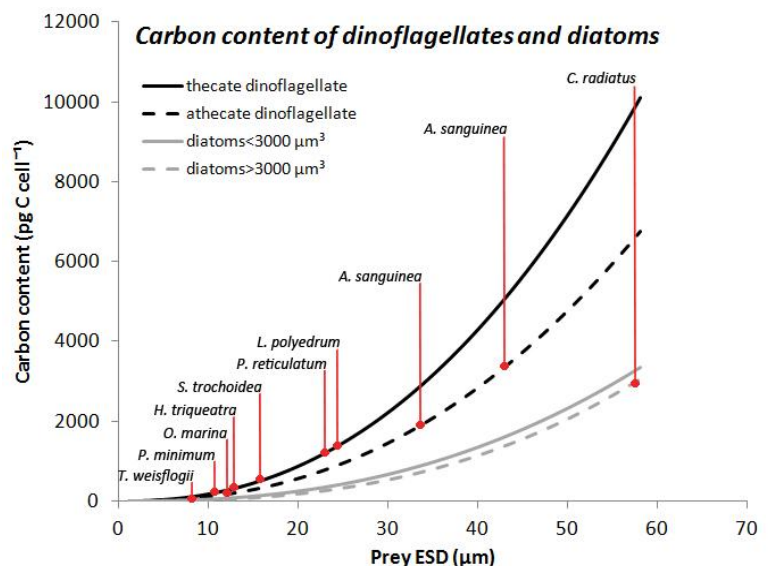


Fig. 9. The average cell size and carbon content of prey species used in this experiment. Carbon content regressions are described in Menden-Deuer and Lessard (2000) for diatoms and dinoflagellates are presented as function of prey size (ESD). For dinoflagellates a distinction was made between 'thecate' and 'athecate' dinoflagellate and for diatoms in cells < 3000 μm^3 and cells > 3000 μm^3 . Cell volume was converted to ESD according to Hansen et al. (1994).

content of large diatom *Coscinodiscus wailessi* that was too large to be entirely ingested by *T. longicornis*. The average size for *C. radiatus* in this experiment was 58.5 μm ESD (measured with the Coulter Counter). However, due to its disc-shape the actual diameter was larger. An average cell diameter of 97 μm was measured under an inverted microscope (Leica DMIL) with an ocular micrometer, which might be too large to fit the copepods mouth. A conservative estimation of mouth size (estimated from the detailed visualization of *T. longicornis* with confocal laser scanning microscopy by Michels and Gorb, 2012) suggest a ratio between prosome length and mouth diameter of an adult female *T. longicornis* equal to 1:18.4. The average copepod size when testing *C. radiatus* was 790 μm (Table 2) which gives an estimated mouth size of 43 μm . This would mean it was not possible to entirely ingest the diatom. With the Coulter Counter only the disappearance of cells in a particular size range were measured, not the actual carbon content of the suspension. In this case many of the diatoms could have been destructed (reduced in size) and not be measured in the measuring range. Therefore the actual carbon ingestion could be overestimated for *C. radiatus*. This inefficient feeding may strongly impact the food web due to an increase in the release of dissolved organic matter (DOC) to the ocean by copepods (Møller, 2005).

The concentration at which the ingestion rate is half the estimated maximum ingestion rate (half saturation constant) can be considered as the capability of to use is food source. In the field, food limitation is seen as the most important factor that limit the copepod to reach its potential maximum feeding rate (Saiz and Calbet, 2007). The capability of *T. longicornis* to use it's food source ($C_{\text{imax}/2}$) appears to be inversely dependent on prey size (Fig. 7B). The copepod reached satiation at a lower prey concentration with increasing prey size as observed for other copepod species (e.g. Frost, 1972; Aisari and Saiz, 2011). Thus *T. longicornis* can satisfy its metabolic demands at relative low carbon concentrations of large cells. Different from findings for other copepods our results suggest an optimum prey size as the half saturation constant first decreases with prey size and then increases for the largest prey *C. radiatus*. As can be seen in Fig. 7B the estimation of the half saturation constant for the dinoflagellate *P. minimum* is much higher than for other prey species. This species is potentially toxic (Gallardo Rodríguez et al., 2009) and might be rejected relatively often by the copepod compared to other prey. However, the half saturation constant for the potential toxic dinoflagellate *P. reticulatum* does not suggest cell rejection.

7.2.2 The effect of prey size on the clearance rate

The prey species selected for this research had a size range from 6.1 to 58.5 μm ESD. This range was rather large compared to other studies focusing on the effect of prey size on the feeding performance of *T. longicornis* (e.g. O'Connors 1980; Gentsch et al., 2009). Although *T. longicornis* is known to be able to feed on smaller (e.g. O'Connors, 1980) and larger prey items (e.g. Jansen, 2008) the selected range covered its theoretical optimal prey-to-predator size ratio. The theoretical optimum for copepods is at a prey-to-predator ratio of 1:18 (± 3) (Hansen et al., 1994). In this study the average copepod length was 858 μm and the average size in ESD was equal to 568 μm . According to the theoretical optimal prey-to-predator size ratio the maximum estimated clearance was expected at prey species of 31.6 μm ESD.

In this study a maximum estimated clearance rate was found for the dinoflagellate *A. sanguinea* with an average size of 33.1 μm ESD. Thereby the upper limit of the prey size spectrum of *T. longicornis* was found, while earlier studies on prey size spectrum of *T. longicornis* were not able to determine

this limit (e.g. O'Connors 1980; Gentsch et al., 2009). As shown in Fig. 8 the estimated maximum clearance rates for *T. longicornis* increased with prey size and a maximum clearance rate was observed for the dinoflagellate *A. sanguinea* (33.1 μm ESD). Then a decrease of clearance rate with prey size was observed (Fig. 7A). This size-dependant clearance pattern resembled a dome-shaped curve as found for other copepods (Berggreen et al., 1988; Hansen et al., 1994) and suggests an optimal prey-to-predator size ratio. The prey size spectrum (Fig. 8) implies an optimal prey-to-predator ratio between 0.055-0.080 (or 1:18.1 – 1:12.5) which is close to the group-specific optimal prey size for copepods of 1:18 as determined by Hansen et al. (1994). A lower limit of the prey size spectrum was not determined in this experiment. The smallest (*R. salina*, 6.1 μm ESD) and largest (*C. radiatus*, 58.5 μm ESD) prey tested were still consumed at a significant rate. Literature shows feeding on smaller prey items by *T. longicornis* and prey items that are far larger than its theoretical optimum. O'Connors et al. (1980) showed ingestion of prey items of 4.8 μm ESD and Weiße (1983) and Jansen (2008) described feeding on prey items up to 350 μm and 380 μm ESD, respectively.

Our findings suggest a considerably higher maximum clearance rate than found in earlier studies. The estimated maximum clearance rate in this study was found for the relative large dinoflagellate *Akashiwo sanguinea* (33.1 μm ESD) of 243.9 mL copepod⁻¹ day⁻¹ when the Holling type II model was fitted and 120.8 mL copepod⁻¹ day⁻¹ when a Holling type III model was fitted. The highest estimated maximum clearance rates for *T. longicornis* in earlier studies were found by Shultz and Kiørboe (2009) of 51.2 mL copepod⁻¹ day⁻¹ feeding on *Gyrodinium instriatum* and 49 mL copepod⁻¹ day⁻¹ feeding on *Balanion comatum* by Jakobsen et al. (2005).

7.3 The feeding performance of *T. longicornis* compared to other marine copepods

To explore the grazing performance of the *T. longicornis* compared to other copepods, the model results of all maximum feeding rates determined in this experiment were compared to the maximum feeding rates of other single prey laboratory-determined feeding rates of marine copepods. However, few studies cover the feeding performance over a wide range of prey sizes. The use of maximum ingestion and clearance rates for different sized prey, as done in this study, could reveal the upper and lower limit in ingestion and clearance rates as a function of copepod size.

Both maximum ingestion and clearance rates for all marine copepods in literature show a positive correlation to the copepods size (in ESD) as shown in Fig 10. Implementing the results from this study, the maximum clearance rates of *T. longicornis* estimated by both a Holling type II and III model show a relative high maximum clearance rate for its size. The estimated maximum ingestion rate for *T. longicornis* are as expected for its size when both a Holling type II and type III model is fitted to the observation, thus the individual copepod could shows an average maximum carbon uptake compared to other marine copepods.

$$\log(F_{\max}) = 2.862 \cdot \log(\text{copepod size}) - 6.294$$

$$r^2 = 0.73 \quad p < 0,01$$

$$\log(I_{\max}) = 2,852 \cdot \log(\text{copepod size})$$

$$r^2 = 0.823 \quad p < 0,01$$

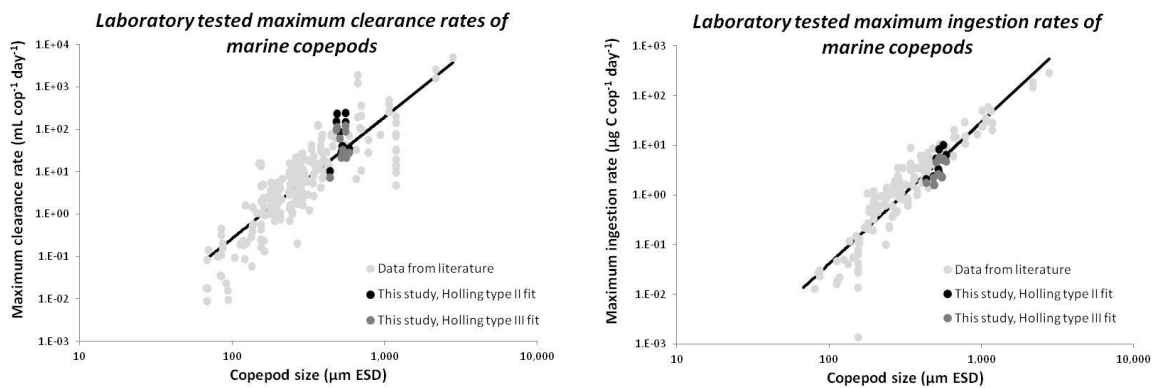


Fig. 10. Laboratory tested maximum clearance (left) and ingestion (right) rates of marine copepods as function of copepod size (ESD in μm). Data from this study is shown for the type II fitted model (black) and type III fitted model (dark grey). A positive correlation between copepod size and clearance/ingestion rates is proved by a Pearson's r test. The linear regression fit for all rates is also given. Data was collected by Kiørboe (unpublished data) and can be found in Appendix II.

7.4 Complications in modeling copepod feeding

Extrapolating laboratory results and models to the in situ carbon uptake should be done with caution. Siaz and Calbet (2010) showed that ingestion rates in field measurements are often lower compared to laboratory determined rates and could be mainly contributed to food limitation in the world's oceans. Thereby natural diet of the copepod could consist of many different prey of several trophic levels. Calanoid copepods do not only eat phytoplankton but have a complex diet (Nejstgaard et al., 2001). This also applies to *T. longicornis*. Although they may have a substantial impact on the phytoplankton standing stock (Gentsch et al., 2009) they are not exclusively herbivorous. Many copepods are able to feed on microzooplankton, copepod eggs and nauplii (Heinle 1970, Daan et al 1988) and in some cases even fish eggs and larvae (Yen, 1987). Copepods often switch to animal prey as energy resource when other food sources are scarce (Heinle 1970, Daan et al 1988). Study by Daan et al. (1988) indicates that *T. longicornis* even show intra-specific predation. They found predation on nauplii by adult *T. longicornis* females, especially at low phytoplankton concentrations.

Copepods are also able to ingest faecal pellets produced by both adults and nauplii, even in the presence of phytoplankton food sources. Faecal pellets of copepods form an important component of the particulate carbon flux through the water column. Ingestion and digestion of faecal pellets may decrease the carbon content by assimilation of organic carbon previously not assimilated (Green et al., 1992) and thus the downward carbon flux.

Feeding on these alternate food sources and prey switching should thus not be neglected in estimating copepod-mediated carbon fluxes and the role of the copepod in the marine carbon cycle depicted in Fig. 1 is in reality thus more complex. The actual grazing on the primary production

estimated by single prey experiments could be lower due to the 'recycling' of carbon by feeding on non-autotrophic food sources, especially when other food sources are scarce.

8. CONCLUSION

The feeding response of zooplankton on the oceans primary production is a fundamental parameter in ecosystem models and the ocean carbon cycle. This study provided extensive information on the role of prey density and prey size on the feeding response of *T. longicornis*, one of the most dominant copepod species in the northern hemisphere.

Feeding experiments on monoalgal diets showed a concentration dependant ingestion and clearance rate of *T. longicornis* for all tested prey sizes. Estimations of the maximum ingestion and clearance rates showed higher rates than previously described in literature. Although this experiment did not conclusively prove what model fitted the observations best, literature suggests the functional response of *T. longicornis* is best described by a Holling type III model (Van Duren, 2000).

Testing the clearance rate of *T. longicornis* for different sized prey showed that the estimated maximum clearance rate is dependant on prey size. An optimal prey-to-predator size ratio was found between 0.055-0.080 (or 1:18.1 – 1:12.5) which is close to the group-specific optimal prey size for copepods of 1:18 (Hansen et al., 1994). *T. longicornis* showed significant consumption of all tested prey sizes and was able to feed on prey much larger than its mouth size.

Although the maximum ingestion rate of *T. longicornis* was not affected by prey size, the capability of *T. longicornis* to use it's food source appeared to be dependent on prey size. Results suggest the copepod reached satiation at a lower prey concentration with increasing prey size up to an optimum prey size.

The study of copepod feeding as function of prey size provided the chance to compare the feeding performance of *T. longicornis* to other marine copepods and showed that *T. longicornis* has a relative high estimated maximum clearance rate for its size and an average estimated maximum carbon uptake.

To fully understand and quantify the role of copepods in the ocean carbon cycle and food web, study on the effect of prey density and prey size on their feeding response is vital. Studies similar to this study are needed for other copepods to increase the accuracy of ecosystem models and models to estimate copepod mediated carbon fluxes. Thereby the effect of complex in situ feeding behavior such as feeding on alternate food sources and 'recycling' of carbon by feeding on non-autotrophic food sources should be taken into account.

REFERENCES

- Almeda, R., Augustin, C.B., Alcaraz, M., Calbet, A., Saiz, E., 2010. Feeding rates and gross growth efficiencies of larval developmental stages of *Oithona davisae* (Copepoda, Cyclopoida). *Journal of Experimental Marine Biology and Ecology*. Volume 387, 24–35
- Altjetlawi, A.A., Sparrevik, E. and Leonardsson, K., 2004. Prey-predator size-dependant functional response: derivation and rescaling to the real world. *Journal of Animal Ecology*. Volume 73, pp 239-252
- Ambler, J.W. and Frost, B.W. The feeding behavior of a predatory planktonic copepod, *Tortanus discaudatus*. *Limnology and Oceanography*. Volume 19, pp 446-451
- Anderson, T.R., Gentleman, W.C., Sinha, B., 2010. Influence of grazing formulation on the emergent properties of a complex ecosystem model in a global general circulation model. *Progress in Oceanography*. Volume 87, pp 201-213
- Berge, T., Hansen, P.J. and Moestrup, Ø., 2008. Prey size spectrum and bioenergetics of the mixotrophic dinoflagellate *Karlodinium armiger*. *Aquatic Microbial Ecology*. Volume 50, pp 289-299
- Berggreen, U., Hansen, B. and Kiørboe, T., 1988. Food size spectra, ingestion and growth of the copepod *Acartia tonsa* during development: implications for determination of copepod production. *Marine Biology*. Volume 99, pp 341-352
- Buesseler K.O. and Lampitt R.S., 2008. Introduction to “Understanding the Ocean’s Biological Pump: results from VERTIGO”. *Deep Sea Research II*. Volume 55, pp 1519-1521
- Conway, D.V.P., 2006. Identification of the copepodite developmental stages of twenty-six North Atlantic copepods. *Occasional Publications. Marine Biological Association of the United Kingdom*. No. 21
- Costa, R.M. and Fernández, F., 2002. Feeding and survival rates of the copepods *Euterpina acutifrons* Dana and *Acartia grani* Sars on the dinoflagellates *Alexandrium minutum* Balech and *Gyrodinium corsicum* Paulmier and the Chryptophyta *Rhodomonas baltica* Karsten. *Journal of Experimental Marine Biology and Ecology*. Volume 273, pp 131-142
- Cox, P.M., Betts, R.A., Jones, C.D., Spall, S.A., Totterdell, I.J., 2000. Acceleration of global warming due to carbon-cycle in a coupled climate model. *Nature*. Volume 408, pp 184-187
- Daan, R., Gonzalez, S.R., Klein Breteler, W.C.M., 1988. Cannibalism in omnivorous calanoid copepods. *Marine Ecology - Progress Series*. Volume 47, pp 45-54
- Dam, H.G. and Petersen, W.T., 1993. Seasonal contrasts in the diel vertical distribution, feeding behavior, and grazing impact of the copepod *Temora longicornis* in Long Island Sound. *Journal of Marine Research*. Volume 51, No. 3, pp 561-594
- DeMott, W.R. and Watson, M.D., 1991. Remote detection of algae by copepods: responses to algal size, odors and motility. *Journal of Plankton Research*. Volume 13, Issue 6, pp 1203-1222

- Drits, A.V. and Semenova, T.N., 1984. Experimental investigation of the feeding of *Oithona similis* Claus. *Oceanology*. Volume 24, pp 755-759
- Duarte, C.M. and Cebrian, J., 1996. The Fate of Marine Autotrophic Production. *Limnology and Oceanography*. Volume 41, Issue 8, pp 1758-1766
- Durbin, E.G., Durbin, A.G., Wlodarczyk, E., 1990. Diel feeding behavior in the marine copepod *Acartia tonsa* in relation to food availability. *Marine Ecology Progress Series*. Volume 68, pp 23-45
- Durbin, E.G., Durbin, A.G., 1992. Effects of temperature and food abundance on grazing and short-term weight change in the marine copepod *Acartia hudsonica*. *Limnology and Oceanography*. Volume 37, pp 361-378
- Dutz, J., 1998. Repression of fecundity in the neritic copepod *Acartia clausi* exposed to the toxic dinoflagellate *Alexandrium lusitanicum*: Relationship between feeding and egg production. *Marine Ecology Progress Series*. Volume 175, pp 97-107
- Falkowski, P.G. and Oliver, J.O., 2007. Mix and match: how climate selects phytoplankton. *Nature Reviews, Microbiology*. Volume 5, pp 813-819
- Fernandez Araos, N.C., 1991. Individual biomass, based on body measures, of copepod species considered as main forage items for fishes of the Argentine shelf. *Oceanologica Acta*. Volume 14, No. 6, pp 575-580
- Fernández, F., 1979. Particle selection in the nauplius of *Calanus pacificus*. *Journal of Plankton Research*. Volume 1, No. 4, pp 313-328
- Frangoulis, C., Christou, E.D., Hecq, J.H., 2005. Comparison of Marine Copepod Outfluxes: Nature, Rate, Fate and Role in the Carbon and Nitrogen Cycles. *Advances in Marine Biology*. Volume 47, pp 253-309
- Frost, B.W., 1972. Effects of size and concentration of food particles on the feeding behavior of the marine planktonic copepod *Calanus Pacificus*. *Limnology and Oceanography*. Volume 17, Issue 6, pp 805-815
- Gallardo Rodríguez, J.J., Sánchez Mirón, A., Cerón García, M.C., Belarbi, E.H., García Camacho, F., Christi, Y., Molina Grima, E., 2009. Macronutrients requirements of the dinoflagellate *Protoceratium reticulatum*. *Harmful Algae*. Volume 8, pp 239-246
- Gentleman, W., Leising, A., Frost, B., Strom, S., Murray, J., 2003. Functional responses for zooplankton feeding on multiple resources: a review of assumptions and biological dynamics. *Deep Sea Research II*. Volume 50, pp 2847-2875
- Gentsch, E., Kreibich, T., Hagen, W., Niehoff, B., 2009. Dietary shifts in the copepod *Temora longicornis* during spring: evidence from stable isotope signatures, fatty acid biomarkers and feeding experiments. *Journal of Plankton Research*. Volume 31, No. 1, pp 45-60
- Green, .E.P., Harris, R.P., Duncan, A., 1992. The production of faecal pellets by nauplii of marine copepods. *Journal of Plankton Research*. Volume 14, No. 12, pp 1631-1643

- Hansen, B. Koefoed Bjornsen, P., Hansen, P.J., 1994. The Size Ration Between Planktonic Predators and Their Prey. *Limnology and Oceanography*. Volume 39, No. 2, pp 395-403
- Hansen, F.C., 1995. Trophic interactions between zooplankton and *Phaeocystis* cf. *globosa*. *Helgoländer Meeresuntersuchungen*. Volume 49, Issue 1-4, pp 283-293
- Hansen, F.C., Witte, H.J. and Passarge, 1996. Grazing in the heterotrophic dinoflagellate *Oxyrrhis marnina*: size selectivity and preference for calcified *Emiliana huxleyi* cells. *Aquatic Microbial Ecology*. Volume 10, pp 307-313
- Harvey, L.D.D., 2000. Global Warming – The Hard Science. Pierson Prentice-Hall, Harlow, United Kingdom
- Heinle, D.R. 1970. Population dynamics of exploited cultures of calanoid copepods. *Helgoländer Meeresuntersuchungen*. Volume 20, pp 360-372
- Henriksen, C. I., Saiz, E., Calbet, A., & Hansen, B. W., 2007. Feeding activity and swimming patterns of *Acartia grani* and *Oithona davisae* nauplii in the presence of motile and non-motile prey. *Marine Ecology Progress Series*. Volume 331, pp 119-129
- Holling, C.S., 1959. Some Characteristics of Simple Types of Predation and Parasitism. *The Canadian Entomologist*. Volume 91, Issue 07, pp 385-398
- Isari, S. and Saiz, E., 2011. Feeding performance of the copepod *Clausocalanus lividus* (Frost and Fleminger, 1968). *Journal of Plankton Research*. Volume 33, No. 5 pp 715-728
- Jakobsen, H.J., Halvorsen, E., Hansen, B.W., Visser. A.W., 2005. Effects of prey motility and concentration of feeding in *Acartia tonsa* and *Temora longicornis*: the importance of feeding modes. *Journal of Plankton Research*. Volume 27, No. 8, pp 775-785
- Jansen, S., 2008. Copepods grazing on *Coscinodiscus wailesii*: a question of size? *Helgoländer Meeresuntersuchungen*. Volume 62, pp 251-255
- Jiang, H. and Kjørboe, T., 2011. The fluid dynamics of swimming by jumping in copepods. *Journal of the Royal Society*. Volume 8, pp 1090-1103
- Kjørboe, T., Møhlenberg, F. and Nicolajsen, H., 1982. Ingestion rate and gut clearance in the planktonic copepod *Centropages hamatus* (Lilljeborg) in relation to food concentration and temperature. *Ophelia*. Volume 21, No. 2, pp 181-194
- Kjørboe, T., 1998. Population regulation and role of mesozooplankton in shaping marine pelagic food webs. *Hydrobiologica*. 363, pp 13-27
- Kjørboe, T., 2008a. A Mechanistic Approach to Plankton Ecology. Princeton University Press, New Jersey
- Kjørboe, T., 2008b. Optimal swimming strategies in mate-searching pelagic copepods. *Oecologia*. Volume 155, pp 179–192

- Klein Breteler, W.C.M. and Gonzales, S.R., 1982. Influence of Cultivation and food Concentration on Body Length of Calanoid Copepods. *Marine Biology*. Volume 71, pp 157-161
- Klein Breteler, W.C.M., Schogt, N. and Gonzales, S.R., 1990. On the role of food quality in grazing and development of life stages, and genetic change of body size during cultivation of pelagic copepods. *Journal of Experimental Marine Biology and Ecology*. Volume 135, Issue 3, pp 177-189
- Klein Breteler, W.C.M. and Koski, M., 2003. Development and grazing of *Temora longicornis* (Copepoda, Calanoida) nauplii during nutrient limited *Phaeocystis globosa* blooms in mesocosms. *Hydrobiologia*. Volume 491, pp 185-192
- Koehl, M.A.R. and Strickler, J.R., 1981. Copepod feeding currents: Food capture at low Reynolds number. *Limnology and Oceanography*. Volume 26, Issue 6, pp 1062-1073
- Koski, M., Dutz, J., Klein Breteler, W.C.M., 2005. Selective grazing of *Temora longicornis* in different stages of a *Phaeocystis globosa* bloom-a mesocosm study. *Harmful Algae*. Volume 4, pp 915-927
- Lampitt, R. S., 1978. Carnivorous feeding by a small marine copepod. *Limnology and Oceanography*. Volume 23, pp 1228–1231
- Lampitt, R. S. and Gamble, J. C., 1982. Diet and respiration of the small planktonic marine copepod *Oithona nana*. *Marine Biology*. Volume 66, pp 185–190
- Lehman, J.T., 1976. The filter feeder as an optimal forager, and the predicted shape of feeding curves. *Limnology and Oceanography*. Volume 21, pp 501-516
- Liu, S. and Wang, W.X., 2002. Feeding and reproductive responses of marine copepods in South China Sea to toxic and nontoxic phytoplankton. *Marine Biology*. Volume 140, pp 595-603
- Martynova, D.M., Graeve, M. and Bathmann, U.V., 2009. Adaptation strategies of copepods (superfamily Centropagoidea) in the White Sea (66°N). *Polar Biology*. Volume 32, Issue 2, pp 133-146
- Menden-Deuer, S. and Lessard, E.J., 2000. Carbon to volume relationships for dinoflagellates, diatoms, and other protist plankton. *Limnology and Oceanography*. Volume 45, Issue 3, pp 569-579
- Michels, J. and Gorb, S.N., 2012. Detailed three-dimensional visualization of resilin in the exoskeleton of arthropods using confocal laser scanning microscopy. *Journal of Microscopy*. Volume 245, pp 1-16
- Møller, E.F., 2005. Sloppy feeding in marine copepods: prey-size-dependent production of dissolved organic carbon. *Journal of Plankton Research*. Volume 27, No. 1, pp 27-35
- Nakamura, Y. and Turner, J. T., 1997. Predation and respiration by the small cyclopoid copepod *Oithona similis*: How important is feeding on ciliates and heterotrophic flagellates? *Journal of Plankton Research*. Volume 19, pp 1275–1288
- Nassogne, A., 1970. Influence of food organisms on the development and culture of pelagic copepods. *Helgoländer Meeresuntersuchungen*. Volume 20, pp333-245

- Nejstgaard, J.C., Båmstedt, U., Bagøien, E., Solberg, P.T., 1995. Algal constraints on copepod grazing. Growth state, toxicity, cell size, and season as regulating factors. *ICES Journal of Marine Science*. Volume 52, pp 347-357
- Nejstgaard, J.C., Naustvoll, L.J., Sazhin, A., 2001. Correcting for underestimation of microzooplankton grazing in bottle incubation experiments with mesozooplankton. *Marine Ecology Progress Series*. Volume 221, pp 59-75
- Nielsen, T.G. and Andersen, C.M., 2002. Plankton community structure and production along a freshwater-influenced Norwegian fjord system. *Marine Biology*. Volume 141, pp 707-724
- Nybakken, J.W., 2001. *Marine Biology – An Ecological Approach*, Fifth Edition. Benjamin Cummings, San Francisco
- O’Connors, Jr., H.B., Biggs, D.C., Ninivaggi, D.V., 1980. Particle-Size-Dependent Maximum Grazing Rates for *Temora longicornis* Fed Natural Particle Assemblages. *Marine Biology*. Volume 56, pp 65-70
- Ölundh, E., 1977. A comparative study of three zooplankton communities on the Swedish west coast with respect to composition, dynamics and function. Department of Zoology, Göteborgs Universitet
- Paffenhöfer, G. A., 1993. On the ecology of marine cyclopoid copepods (Crustacea, Copepoda). *Journal of Plankton Research*. Volume 15, pp 37–55
- Real, L.A., 1977. The Kinetics of Functional Response. *The American Naturalist*. Volume 111, No. 978, pp 289-300
- Rey, C., Harris, R., Irigoien, X., Head, R., Carlotti, F., 2001. Influence of algal diet on growth and ingestion of *Calanus helgolandicus* nauplii. *Marine Ecology Progress Series*. Volume 216, pp 151
- Rey-Rassat, C., Irigoien, X., Harris, R., Head, R., Carlotti, F., 2002a. Growth and development of *Calanus helgolandicus* reared in the laboratory. *Marine Ecology Progress Series*. Volume 238, pp 125-138
- Rey-Rassat, C., Irigoien, X., Harris, R., Head, R., Carlotti, F., 2002b. Egg production rates of *Calanus helgolandicus* females reared in the laboratory: variability due to present and past feeding conditions. *Marine Ecology Progress Series*. Volume 238, pp 139-151
- Robertson, S.B. and Frost, B.W., 1977. Feeding by an omnivorous planktonic copepod *Aetideus divergens* Bradford. *Journal of Experimental Marine Biology and Ecology*. Volume 29, pp 231-24
- Sabine, C.L., Feely, R.A., Gruber N., Key, R.M., Lee, K., Bullister, J.L., Wanninkhof, R., Wong, C.S., Wallace, D.W.R., Tilbrook, B., Miller, F.J., Peng, T.H., Kozyr, A., Ono, T., Rios, A.F., 2004. The Oceanic Sink for Anthropogenic CO₂. *Science*. Volume 205, No 5682, pp 367-371
- Saiz, E. and Calbet, A., 2007. Scaling of feeding in marine calanoid copepods. *Limnology and Oceanography*. Volume 52, Issue 2, pp 668-675
- Saiz, E. and Calbet, A., 2011. Copepod feeding in the ocean: scaling patterns, composition of their diet and the bias of estimates due to microzooplankton grazing during incubations. *Hydrobiologica*. Volume 666, pp 181-196

- Saiz, E., Calbet, A., Broglio, E., 2003. Effects of small-scale turbulence on copepods: The case of *Oithona davisae*. *Limnology and Oceanography*. Volume 48, pp 1304-1311
- Saiz, E. and Kiørboe, T., 1995. Predatory and suspension feeding of the copepod *Acartia tonsa* in turbulent environments. *Marine Ecology Progress Series*. Volume 122, pp 147–158
- Sars, G.O., 1901. An Account of the Crustacea of Norway, with short descriptions and figures of all the species. Volume IV, Copepoda Calanoida. Published by the Bergen Museum
- Sautour, B. and Castel, J., 1993. Feeding behaviour of the coastal copepod *Euterpina acutifrons* on small particles. *Cahiers de Biologie Marine*. Volume 34, pp 239-251
- Schultz, M. and Kiørboe, T., 2009. Active prey selection in two pelagic copepods feeding on potentially toxic and non-toxic dinoflagellates. *Journal of Plankton Research*. Volume 31, No. 5, pp 553-561
- Smith, R.L. and Smith, T.M., 2003. *Elements of Ecology*, Fifth Edition. Benjamin Cummings, San Francisco
- Støttrup, J. and Jensen, J. 1990. Influence of algal diet on feeding and egg-production of the calanoid copepod *Acartia tonsa* Dana. *Journal of Experimental Marine Biology and Ecology*. Volume 141, No. 2-3, pp 87-105
- Teegarden, G. J., 1999. Copepod grazing selection and particle discrimination on the basis of PSP toxin content. *Marine Ecology Progress Series*. Volume 181, pp 163–176.
- Uye, S., 1986. Impact of copepod grazing on the red-tide flagellate *Chattonella antiqua*. *Marine Biology*. Volume 92, Issue 1, pp 35-43
- Uye, S. and Kayano, Y., 1994. Predatory feeding behavior of *Tortanus* (Copepod: Calanoida): life-stage differences and the predation impact on small planktonic crustaceans. *Journal of Crustacean Biology*. Volume 14, No. 3, pp 473-483
- Van Duren, L.A., 2000. Moving (in) Water – Behavioral kinematics, energetic and hydrodynamics of the calanoid copepod *Temora longicornis*. Rijksuniversiteit Groningen
- Veloza, A.J., Chu, F.L.E. and Tang, K.W., 2006. Trophic modification of essential fatty acids by heterotrophic protists and its effect on the fatty acid composition of the copepod *Acartia tonsa*. *Marine Biology*. Volume 148, pp 779-788
- Vincent, D. and Hartmann, H.J., 2001. Contribution of ciliated microprotozoans and dinoflagellates to the diet of three copepod species in the Bay of Biscay. *Hydrobiologia*. Volume 443, pp 193–204
- Weiße, T., 1983. Feeding of calanoid copepods in relation to *Phaeocystis pouchetii* blooms in the German Wadden Sea area off Sylt. *Marine Biology*. Volume 74, pp 87-94
- Wetzel, R.G. and Likens, G.E., 2003. *Limnological Analyses*, Third Edition. Springer, United States of America

Williams, R.G. and Follows, M.J., 2011. *Ocean Dynamics and the Carbon Cycle*. Cambridge University Press

Yen, J., 1985. Selective predation by the carnivorous marine copepod *Euchaeta elongata*: Laboratory measurements of predation rates verified by field observations of temporal and spatial feeding patterns. *Limnology and Oceanography*. Volume 30, pp 577–597

Yen, J., 1987. Predation by carnivorous marine copepod, *Euchaeta norvegica* Boeck, on eggs and larvae of the North Atlantic cod *Gadus morhua* L. *Journal of Experimental Marine Biology and Ecology*. Volume 112, pp 283-296

Zamora-Terol, S. and Saiz, E., 2013. Effects of food concentration on egg production and feeding rates of the cyclopoid copepod *Oithona davisae*. *Limnology and Oceanography*. Volume 58, pp 376-387

APPENDIX I Results of bottle incubation experiments and statistical analysis of observations.

Overview of the average measured prey concentrations ($\mu\text{g C mL}^{-1} \times 10^5$) during each experiment and the average ingestion ($\mu\text{g C cop}^{-1} \text{ day}^{-1}$) and clearance rates ($\text{mL cop}^{-1} \text{ day}^{-1}$) with one standard error. The difference in cell concentration between control bottles and experimental bottles were tested on significance by a independent samples student t-test (one-tailed and no equal variances assumed). At some concentrations the amount of bottles was not sufficient to prove significant cell consumption

Prey species	Prey concentration ($\mu\text{g C mL}^{-1} \times 10^5$)	Ingestion rate ($\mu\text{g C cop}^{-1} \text{ day}^{-1} \times 10^5$)	Clearance rate ($\text{mL cop}^{-1} \text{ day}^{-1}$)	<i>n</i>		Sign.
				control bottles	exp. bottles	
<i>R. salina</i>	0.37 ± 0.00	3.10 ± 0.16	8.45 ± 0.53	3	2	0.03
	0.66 ± 0.01	5.23 ± 1.41	7.90 ± 2.18	3	3	0.02
	1.18 ± 0.01	6.05 ± 1.49	5.17 ± 1.32	3	3	0.02
	2.05 ± 0.01	12.58 ± 0.55	6.13 ± 0.27	3	3	0.00
	3.81 ± 0.01	13.33 ± 1.42	3.51 ± 0.39	3	3	0.00
	6.75 ± 0.02	15.87 ± 1.71	2.35 ± 0.26	2	3	0.02
<i>L. polyedrum</i>	0.16 ± 0.01	13.10 ± 1.14	85.50 ± 12.65	3	3	0.01
	0.27 ± 0.01	20.15 ± 1.61	75.73 ± 10.07	3	3	0.00
	0.34 ± 0.01	31.84 ± 1.09	93.76 ± 3.47	3	3	0.00
	0.97 ± 0.02	34.90 ± 3.25	36.14 ± 4.01	3	3	0.00
	1.66 ± 0.01	48.42 ± 0.49	29.15 ± 0.42	3	3	0.00
	3.52 ± 0.08	46.60 ± 7.07	13.34 ± 2.23	3	3	0.01
<i>H. triquetra</i>	0.19 ± 0.01	4.47 ± 0.89	23.75 ± 5.31	3	3	0.04
	0.27 ± 0.00	2.96 ± 0.52	10.85 ± 2.04	3	3	0.09
	0.48 ± 0.01	10.29 ± 0.78	21.68 ± 1.82	3	3	0.00
	0.79 ± 0.02	20.48 ± 1.47	26.09 ± 2.45	3	3	0.01
	1.30 ± 0.06	34.06 ± 5.64	26.67 ± 5.37	3	3	0.02
	2.66 ± 0.05	35.31 ± 1.78	13.32 ± 0.89	3	3	0.02
<i>P. minimum</i>	0.23 ± 0.01	3.78 ± 1.74	17.44 ± 8.42	3	3	0.05
	0.37 ± 0.00	4.75 ± 0.39	13.03 ± 1.20	3	3	0.00
	0.59 ± 0.02	11.64 ± 2.46	20.15 ± 4.76	3	3	0.02
	1.03 ± 0.01	21.85 ± 1.14	21.24 ± 1.21	3	3	0.00
	1.77 ± 0.02	29.78 ± 2.04	16.86 ± 1.32	3	3	0.00
	3.16 ± 0.01	41.91 ± 3.33	13.28 ± 1.11	3	3	0.00
<i>A. sanguinea (33.1 μm)</i>	0.07 ± 0.00	6.72 ± 0.53	91.43 ± 10.27	3	3	0.00
	0.16 ± 0.02	15.83 ± 4.06	107.47 ± 34.16	3	3	0.02
	0.25 ± 0.03	15.54 ± 3.35	65.97 ± 18.73	3	3	0.01
	0.48 ± 0.03	22.79 ± 3.19	48.74 ± 8.79	3	3	0.00
	0.99 ± 0.02	22.92 ± 1.45	23.25 ± 1.93	3	3	0.00
	1.79 ± 0.02	18.19 ± 1.81	10.17 ± 1.12	3	3	0.06
<i>S. trochoidea</i>	0.20 ± 0.00	3.31 ± 0.22	16.31 ± 1.26	3	3	0.01
	0.35 ± 0.01	6.05 ± 0.86	17.44 ± 2.74	3	3	0.05
	0.57 ± 0.01	15.22 ± 0.77	26.60 ± 1.42	3	3	0.00
	0.98 ± 0.03	21.57 ± 2.47	22.27 ± 3.07	3	3	0.03
	1.89 ± 0.05	15.03 ± 5.78	8.11 ± 3.22	3	3	0.29
	3.40 ± 0.04	24.27 ± 3.57	7.18 ± 1.13	3	3	0.06
<i>O. marina</i>	0.19 ± 0.00	6.06 ± 0.64	31.47 ± 4.17	3	3	0.01
	0.31 ± 0.01	9.53 ± 1.62	31.41 ± 6.03	3	3	0.00
	0.52 ± 0.02	14.49 ± 2.14	28.21 ± 5.17	3	3	0.00
	0.86 ± 0.01	26.64 ± 1.54	31.06 ± 2.07	3	3	0.00
	1.54 ± 0.03	34.91 ± 2.24	22.66 ± 1.84	3	3	0.00
	2.86 ± 0.04	47.16 ± 3.96	16.53 ± 1.63	3	3	0.00

APPENDIX I Continued.

Prey species	Prey concentration (pg C mL ⁻¹ x 10 ⁵)	Ingestion rate (pg C cop ⁻¹ day ⁻¹ x 10 ⁵)	Clearance rate (mL cop ⁻¹ day ⁻¹)	<i>n</i>		Sign.
				control bottles	exp. bottles	
<i>T. weisflogii</i>	0.16 ± 0.00	4.54 ± 0.15	28.28 ± 1.33	3	3	0.00
	0.34 ± 0.00	4.88 ± 0.47	14.59 ± 1.56	3	3	0.00
	0.51 ± 0.01	11.62 ± 1.30	22.74 ± 2.86	3	3	0.00
	0.93 ± 0.02	14.78 ± 2.42	16.01 ± 3.01	3	3	0.01
	1.69 ± 0.01	20.52 ± 0.82	12.15 ± 0.55	3	3	0.00
	2.74 ± 0.02	22.44 ± 1.55	8.19 ± 0.57	3	3	0.00
<i>P. reticulatum</i>	0.13 ± 0.00	7.84 ± 0.31	60.23 ± 3.51	3	3	0.06
	0.23 ± 0.01	16.00 ± 0.60	69.83 ± 5.00	3	3	0.01
	0.36 ± 0.01	17.25 ± 1.39	47.92 ± 5.48	3	3	0.00
	0.71 ± 0.03	23.03 ± 3.04	33.06 ± 6.14	3	3	0.01
	1.20 ± 0.01	46.25 ± 2.27	38.45 ± 2.26	3	3	0.00
	2.44 ± 0.03	38.16 ± 2.65	15.65 ± 1.26	3	3	0.00
<i>A. sanguinea (42.4 μm)</i>	0.07 ± 0.00	4.52 ± 0.89	69.55 ± 16.97	3	3	0.04
	0.10 ± 0.01	10.96 ± 0.69	113.72 ± 12.73	3	3	0.00
	0.20 ± 0.01	12.91 ± 1.08	65.11 ± 8.50	3	3	0.00
	0.41 ± 0.01	15.84 ± 1.29	38.99 ± 4.42	3	3	0.00
	0.83 ± 0.02	14.35 ± 2.07	17.47 ± 2.86	3	3	0.01
	1.61 ± 0.02	13.40 ± 2.15	8.35 ± 1.44	3	3	0.01
<i>C. radiatus</i>	0.07 ± 0.00	8.64 ± 0.24	121.29 ± 2.41	3	3	0.00
	0.13 ± 0.01	9.43 ± 1.89	74.42 ± 20.39	3	3	0.02
	0.25 ± 0.01	14.84 ± 1.93	59.97 ± 10.03	3	3	0.00
	0.48 ± 0.03	18.56 ± 2.64	39.24 ± 7.41	3	3	0.01
	1.04 ± 0.03	17.13 ± 2.70	16.54 ± 3.01	3	3	0.01
	1.95 ± 0.04	24.77 ± 4.38	12.82 ± 2.45	3	3	0.00

APPENDIX II Dataset clearance and ingestion rates marine copepods from literature. Clearance and ingestion rates of different size marine copepods from literature are compiled by Kiørboe. Ingestion and clearance rates are corrected to the experimental temperature of this study (14°C). Copepod ESD is calculated from carbon content according to Hansen et al. (1994).

Copepod species	Order	Prey species	Copepod ESD (µm)	Prey ESD (µm)	Maximum ingestion rate (µg C cop ⁻¹ d ⁻¹)	Maximum clearance rate (mL cop ⁻¹ d ⁻¹)	Source
<i>Acartia tonsa</i>	Calanoid	<i>Strombidium sulcatum</i>	362	23	2.3	121.6	Saiz and Kiørboe, 1995
<i>Acartia tonsa</i>	Calanoid	<i>Thalassiosira weissflogii</i>	362	14	2.1	125.6	Saiz and Kiørboe, 1995
<i>Tortanus discoudatus</i>	Calanoid	<i>Calanus pacificus</i> NIII	660	172	14.4	1225.4	Ambler and Frost, 1974
<i>Tortanus discoudatus</i>	Calanoid	<i>Calanus pacificus</i> NV	660	228	20.1	1874.0	Ambler and Frost, 1974
<i>Temora longicornis</i>	Calanoid	<i>Oxhyrris marina</i>	374	13	3.5	-	Klein Breteler et al., 1990 (Saiz et al., 2007)
<i>Temora longicornis</i>	Calanoid	<i>Oxhyrris marina</i>	399	13	6.1	-	Klein Breteler et al., 1990 (Saiz et al., 2007)
<i>Temora longicornis</i>	Calanoid	<i>Oxhyrris marina</i>	478	13	4.1	-	Klein Breteler et al., 1990 (Saiz et al., 2007)
<i>Temora longicornis</i>	Calanoid	<i>Oxhyrris marina</i>	519	13	8.2	-	Klein Breteler et al., 1990 (Saiz et al., 2007)
<i>Acartia tonsa</i>	Calanoid	<i>Thalassiosira weissflogii</i>	474	-	5.4	-	Durbin et al., 1990
<i>Acartia tonsa</i>	Calanoid	<i>Thalassiosira weissflogii</i>	423	-	5.3	-	Durbin et al., 1990
<i>Acartia tonsa</i>	Calanoid	<i>Thalassiosira weissflogii</i>	389	-	-	72.7	Durbin et al., 1990
<i>Acartia hudsonica</i>	Calanoid	<i>Thalassiosira constricta</i>	476	-	8.4	59.4	Durbin and Durbin, 1992
<i>Acartia hudsonica</i>	Calanoid	<i>Thalassiosira constricta</i>	455	-	4.0	38.7	Durbin and Durbin, 1992
<i>Acartia hudsonica</i>	Calanoid	<i>Thalassiosira constricta</i>	412	-	3.9	29.5	Durbin and Durbin, 1992
<i>Acartia hudsonica</i>	Calanoid	<i>Thalassiosira constricta</i>	395	17	3.4	18.9	Durbin and Durbin, 1992
<i>Acartia clausi</i>	Calanoid	<i>Rhodomonas baltica</i>	430	7	5.0	7.2	Dutz, 1998
<i>Acartia clausi</i>	Calanoid	<i>Alexandrium lusitanicum</i>	430	19	5.8	13.5	Dutz, 1998
<i>Calanus pacificus</i>	Calanoid	<i>Thalassiosira weissflogii</i>	183	12	0.5	1.4	Fernández, 1979
<i>Calanus pacificus</i>	Calanoid	<i>Gymnodinium splendens</i>	183	30	0.5	1.4	Fernández, 1979
<i>Calanus pacificus</i>	Calanoid	<i>Gonyaulax polyedra</i>	183	35	0.5	1.4	Fernández, 1979
<i>Calanus pacificus</i>	Calanoid	<i>Chlamydomonas sp</i>	197	11	0.3	1.7	Fernández, 1979
<i>Calanus pacificus</i>	Calanoid	<i>Thalassiosira weissflogii</i>	197	12	0.5	3.0	Fernández, 1979
<i>Calanus pacificus</i>	Calanoid	<i>Peridinium trochoideum</i>	197	18	0.4	4.8	Fernández, 1979
<i>Calanus pacificus</i>	Calanoid	<i>Lauderia borealis</i>	197	29	1.2	5.5	Fernández, 1979
<i>Calanus pacificus</i>	Calanoid	<i>Gymnodinium splendens</i>	197	30	0.7	3.7	Fernández, 1979
<i>Calanus pacificus</i>	Calanoid	<i>Isochrysis galbana</i>	236	4	0.1	0.7	Fernández, 1979
<i>Calanus pacificus</i>	Calanoid	<i>Chlamydomonas sp</i>	236	11	-	1.4	Fernández, 1979
<i>Calanus pacificus</i>	Calanoid	<i>Thalassiosira weissflogii</i>	236	12	0.8	8.6	Fernández, 1979
<i>Calanus pacificus</i>	Calanoid	<i>Peridinium trochoideum</i>	236	18	1.0	2.9	Fernández, 1979
<i>Calanus pacificus</i>	Calanoid	<i>Lauderia borealis</i>	236	29	1.0	15.3	Fernández, 1979
<i>Calanus pacificus</i>	Calanoid	<i>Gymnodinium splendens</i>	236	30	0.9	9.9	Fernández, 1979
<i>Calanus pacificus</i>	Calanoid	<i>Gonyaulax polyedra</i>	236	35	0.8	7.9	Fernández, 1979
<i>Calanus pacificus</i>	Calanoid	<i>Isochrysis galbana</i>	265	4	0.4	0.2	Fernández, 1979
<i>Calanus pacificus</i>	Calanoid	<i>Chlamydomonas sp</i>	265	11	1.1	1.7	Fernández, 1979
<i>Calanus pacificus</i>	Calanoid	<i>Thalassiosira weissflogii</i>	265	12	1.2	8.0	Fernández, 1979
<i>Calanus pacificus</i>	Calanoid	<i>Lauderia borealis</i>	265	29	1.5	16.2	Fernández, 1979
<i>Calanus pacificus</i>	Calanoid	<i>Gymnodinium splendens</i>	265	30	1.3	14.4	Fernández, 1979
<i>Calanus pacificus</i>	Calanoid	<i>Chlamydomonas sp</i>	288	11	0.9	3.2	Fernández, 1979
<i>Calanus pacificus</i>	Calanoid	<i>Thalassiosira weissflogii</i>	288	12	1.9	7.8	Fernández, 1979
<i>Calanus pacificus</i>	Calanoid	<i>Lauderia borealis</i>	288	29	1.5	26.6	Fernández, 1979
<i>Calanus pacificus</i>	Calanoid	<i>Gymnodinium splendens</i>	288	30	1.7	11.5	Fernández, 1979
<i>Calanus pacificus</i>	Calanoid	<i>Coscinodiscus angustii</i>	1067	37	34.5	255.0	Frost, 1992
<i>Calanus pacificus</i>	Calanoid	<i>Coscinodiscus eccentricus</i>	1067	49	28.6	368.8	Frost, 1992
<i>Calanus pacificus</i>	Calanoid	<i>Centric diatom</i>	1067	67	32.5	487.1	Frost, 1992
<i>Calanus sinicus</i>	Calanoid	<i>Alexandrium tamarense</i> ARC101	782	-	14.9	54.9	Liu and Wang, 2002
<i>Calanus sinicus</i>	Calanoid	<i>Alexandrium tamarense</i> CCMP1771	782	-	10.8	28.1	Liu and Wang, 2002
<i>Calanus sinicus</i>	Calanoid	<i>Thalassiosira weissflogii</i>	782	-	-	27.8	Liu and Wang, 2002
<i>Paracalanus crassirostris</i>	Calanoid	<i>Alexandrium tamarense</i> ARC101	405	-	1.8	9.4	Liu and Wang, 2002
<i>Paracalanus crassirostris</i>	Calanoid	<i>Alexandrium tamarense</i> CCMP1771	405	-	1.7	8.9	Liu and Wang, 2002
<i>Paracalanus crassirostris</i>	Calanoid	<i>Thalassiosira weissflogii</i>	405	-	-	10.3	Liu and Wang, 2002
<i>Calanus finmarchicus</i>	Calanoid	<i>Emiliana huxley 92</i>	1183	5	-	4.7	Nejstgaard et al., 1995
<i>Calanus finmarchicus</i>	Calanoid	<i>Emiliana huxley 93</i>	1183	4	-	12.3	Nejstgaard et al., 1995
<i>Calanus finmarchicus</i>	Calanoid	<i>Emiliana huxley 94</i>	1183	4	-	30.9	Nejstgaard et al., 1995
<i>Calanus finmarchicus</i>	Calanoid	<i>Prymnesium patelliferum 92</i>	1183	6	-	14.0	Nejstgaard et al., 1995
<i>Calanus finmarchicus</i>	Calanoid	<i>Thalassiosira nordenskiöldii 92</i>	1183	14	-	138.8	Nejstgaard et al., 1995
<i>Calanus finmarchicus</i>	Calanoid	<i>Thalassiosira nordenskiöldii 93</i>	1183	17	-	196.0	Nejstgaard et al., 1995
<i>Calanus finmarchicus</i>	Calanoid	<i>Chaetoceros calcitrans 93</i>	1183	3	-	18.7	Nejstgaard et al., 1995
<i>Calanus finmarchicus</i>	Calanoid	<i>Pavlova lutheri 93</i>	1183	5	-	9.3	Nejstgaard et al., 1995
<i>Calanus finmarchicus</i>	Calanoid	<i>Rhodomonas baltica</i>	1183	8	-	68.3	Nejstgaard et al., 1995
<i>Calanus finmarchicus</i>	Calanoid	<i>Rhodomonas baltica</i>	1183	8	27.6	74.5	Nejstgaard et al., 1995
<i>Calanus finmarchicus</i>	Calanoid	<i>Emiliana huxley 94</i>	1183	4	20.1	32.1	Nejstgaard et al., 1995
<i>Calanus helgolandicus</i>	Calanoid	<i>Rhodomonas baltica</i>	197	8	0.4	-	Rey et al., 2001
<i>Calanus helgolandicus</i>	Calanoid	<i>Isochrysis galbana</i>	197	5	0.5	-	Rey et al., 2001
<i>Calanus helgolandicus</i>	Calanoid	<i>Prorocentrum micans</i>	195	27	1.1	-	Rey et al., 2001
<i>Calanus helgolandicus</i>	Calanoid	<i>Pleurochrysis carterae</i>	178	10	1.1	-	Rey et al., 2001
<i>Calanus helgolandicus</i>	Calanoid	<i>Thalassiosira weissflogii</i>	198	13	0.8	-	Rey et al., 2001
<i>Calanus helgolandicus</i>	Calanoid	<i>Rhodomonas baltica</i>	213	8	0.6	-	Rey et al., 2001
<i>Calanus helgolandicus</i>	Calanoid	<i>Isochrysis galbana</i>	233	5	0.6	-	Rey et al., 2001
<i>Calanus helgolandicus</i>	Calanoid	<i>Prorocentrum micans</i>	235	27	1.1	-	Rey et al., 2001
<i>Calanus helgolandicus</i>	Calanoid	<i>Pleurochrysis carterae</i>	217	10	0.9	-	Rey et al., 2001
<i>Calanus helgolandicus</i>	Calanoid	<i>Thalassiosira weissflogii</i>	238	13	1.4	-	Rey et al., 2001
<i>Calanus helgolandicus</i>	Calanoid	<i>Rhodomonas baltica</i>	296	8	1.1	-	Rey et al., 2001
<i>Calanus helgolandicus</i>	Calanoid	<i>Isochrysis galbana</i>	278	5	0.5	-	Rey et al., 2001
<i>Calanus helgolandicus</i>	Calanoid	<i>Prorocentrum micans</i>	272	27	1.1	-	Rey et al., 2001
<i>Calanus helgolandicus</i>	Calanoid	<i>Pleurochrysis carterae</i>	253	10	1.0	-	Rey et al., 2001
<i>Calanus helgolandicus</i>	Calanoid	<i>Thalassiosira weissflogii</i>	270	13	1.8	-	Rey et al., 2001
<i>Calanus helgolandicus</i>	Calanoid	<i>Rhodomonas baltica</i>	329	8	0.7	-	Rey et al., 2001
<i>Calanus helgolandicus</i>	Calanoid	<i>Isochrysis galbana</i>	328	5	0.7	-	Rey et al., 2001
<i>Calanus helgolandicus</i>	Calanoid	<i>Prorocentrum micans</i>	291	27	1.4	-	Rey et al., 2001
<i>Calanus helgolandicus</i>	Calanoid	<i>Pleurochrysis carterae</i>	296	10	0.8	-	Rey et al., 2001
<i>Calanus helgolandicus</i>	Calanoid	<i>Thalassiosira weissflogii</i>	314	13	1.6	-	Rey et al., 2001
<i>Calanus helgolandicus</i>	Calanoid	<i>Prorocentrum micans</i>	303	27	3.5	-	Rey-Rassat et al., 2002a
<i>Calanus helgolandicus</i>	Calanoid	<i>Prorocentrum micans</i>	405	27	5.4	-	Rey-Rassat et al., 2002a
<i>Calanus helgolandicus</i>	Calanoid	<i>Prorocentrum micans</i>	530	27	10.5	-	Rey-Rassat et al., 2002a
<i>Calanus helgolandicus</i>	Calanoid	<i>Prorocentrum micans</i>	771	27	29.3	-	Rey-Rassat et al., 2002a
<i>Calanus helgolandicus</i>	Calanoid	<i>Prorocentrum micans</i>	1011	27	24.0	-	Rey-Rassat et al., 2002a

APPENDIX II Continued.

Copepod species	Order	Prey species	Copepod ESD (μm)	Prey ESD (μm)	Maximum ingestion rate ($\mu\text{g C cop}^{-1} \text{d}^{-1}$)	Maximum clearance rate ($\text{mL cop}^{-1} \text{d}^{-1}$)	Source
<i>Calanus helgolandicus</i>	Calanoid	<i>Prorocentrum micans</i>	1155	27	49.0	-	Rey-Rassat et al., 2002a
<i>Calanus helgolandicus</i>	Calanoid	<i>Prorocentrum micans</i>	1013	27	49.3	-	Rey-Rassat et al., 2002b
<i>Calanus helgolandicus</i>	Calanoid	<i>Prorocentrum micans</i>	1100	27	58.7	-	Rey-Rassat et al., 2002b
<i>Aetideus divergens</i>	Calanoid	<i>Thalassiosira fluviatilis</i>	696	13	-	10.6	Robertson and Frost, 1977
<i>Aetideus divergens</i>	Calanoid	<i>Coscinodiscus angatii</i>	696	49	-	99.7	Robertson and Frost, 1977
<i>Aetideus divergens</i>	Calanoid	<i>Coscinodiscus angatii</i>	696	108	-	205.2	Robertson and Frost, 1977
<i>Aetideus divergens</i>	Calanoid	<i>Artemaia nauplii</i>	696	-	-	355.2	Robertson and Frost, 1977
<i>Acartia tonsa femal</i>	Calanoid	<i>Isochrysis galbana</i>	340	5	8.7	2.7	Støttrup and Jensen, 1990
<i>Acartia tonsa femal</i>	Calanoid	<i>Dunaliella tertiolecta</i>	340	7	3.2	8.7	Støttrup and Jensen, 1990
<i>Acartia tonsa femal</i>	Calanoid	<i>Rhodomonas baltica</i>	340	8	4.3	8.1	Støttrup and Jensen, 1990
<i>Acartia tonsa femal</i>	Calanoid	<i>Thalassiosira weissflogii</i>	340	14	3.8	22.6	Støttrup and Jensen, 1990
<i>Acartia tonsa femal</i>	Calanoid	<i>Ditylum brightwellii</i>	340	27	3.2	15.6	Støttrup and Jensen, 1990
<i>Centropages hamatus</i>	Calanoid	<i>Mixed dinoflagellates</i>	540	26	7.7	-	Teegarden, 1999
<i>Eurytemora herdmani</i>	Calanoid	<i>Mixed dinoflagellates</i>	492	27	4.8	-	Teegarden, 1999
<i>Acartia tonsa</i>	Calanoid	<i>Mixed dinoflagellates</i>	405	28	4.9	-	Teegarden, 1999
<i>Acartia Erythraea</i>	Calanoid	<i>Chattonella antiqua</i>	417	-	3.1	17.1	Uye, 1986
<i>Calanus sinicus</i>	Calanoid	<i>Chattonella antiqua</i>	937	-	16.3	74.3	Uye, 1986
<i>Centropages yamadaui</i>	Calanoid	<i>Chattonella antiqua</i>	534	-	5.0	35.2	Uye, 1986
<i>Paracalanus parvus</i>	Calanoid	<i>Chattonella antiqua</i>	350	-	1.6	10.8	Uye, 1986
<i>Pseudocalanus marinus</i>	Calanoid	<i>Chattonella antiqua</i>	419	-	2.2	14.6	Uye, 1986
<i>Tortanus spp</i>	Calanoid	<i>Oithona davisae CV-VI</i>	259	156	0.4	20.9	Uye and Kayano, 1994
<i>Tortanus spp</i>	Calanoid	<i>Oithona davisae CV-VI</i>	328	156	0.6	33.6	Uye and Kayano, 1994
<i>Tortanus spp</i>	Calanoid	<i>Oithona davisae CV-VI</i>	378	156	1.0	31.8	Uye and Kayano, 1994
<i>Tortanus spp</i>	Calanoid	<i>Oithona davisae CV-VI</i>	447	156	1.4	70.5	Uye and Kayano, 1994
<i>Tortanus spp</i>	Calanoid	<i>Oithona davisae CV-VI</i>	259	156	0.6	18.9	Uye and Kayano, 1994
<i>Tortanus spp</i>	Calanoid	<i>Oithona davisae CV-VI</i>	328	156	0.9	42.7	Uye and Kayano, 1994
<i>Tortanus spp</i>	Calanoid	<i>Oithona davisae CV-VI</i>	378	156	1.3	40.0	Uye and Kayano, 1994
<i>Tortanus spp</i>	Calanoid	<i>Oithona davisae CV-VI</i>	447	156	1.7	75.5	Uye and Kayano, 1994
<i>Euchaete elongata</i>	Calanoid	<i>Pseudocalanus sp F</i>	2162	-	184.7	2550.7	Yen, 1985
<i>Euchaete elongata</i>	Calanoid	<i>Acartia clausii</i>	2162	-	147.3	1580.3	Yen, 1985
<i>Euchaete norvegica</i>	Calanoid	<i>Larval cod</i>	2777	731	281.7	4850.7	Yen, 1987
<i>Acartia tonsa</i>	Calanoid	<i>Pavlova lutheri</i>	68	4	-	0.1	Berggreen et al., 1988
<i>Acartia tonsa</i>	Calanoid	<i>Pavlova lutheri</i>	85	4	-	0.3	Berggreen et al., 1988
<i>Acartia tonsa</i>	Calanoid	<i>Pavlova lutheri</i>	137	4	-	0.6	Berggreen et al., 1988
<i>Acartia tonsa</i>	Calanoid	<i>Pavlova lutheri</i>	167	4	-	2.4	Berggreen et al., 1988
<i>Acartia tonsa</i>	Calanoid	<i>Pavlova lutheri</i>	242	4	-	1.3	Berggreen et al., 1988
<i>Acartia tonsa</i>	Calanoid	<i>Pavlova lutheri</i>	270	4	-	2.9	Berggreen et al., 1988
<i>Acartia tonsa</i>	Calanoid	<i>Pavlova lutheri</i>	207	4	-	4.0	Berggreen et al., 1988
<i>Acartia tonsa</i>	Calanoid	<i>Pavlova lutheri</i>	192	4	-	4.6	Berggreen et al., 1988
<i>Acartia tonsa</i>	Calanoid	<i>Pavlova lutheri</i>	242	4	-	7.3	Berggreen et al., 1988
<i>Acartia tonsa</i>	Calanoid	<i>Pavlova lutheri</i>	265	4	-	7.0	Berggreen et al., 1988
<i>Acartia tonsa</i>	Calanoid	<i>Pavlova lutheri</i>	372	4	-	12.3	Berggreen et al., 1988
<i>Acartia tonsa</i>	Calanoid	<i>Isochrysis galbana</i>	68	5	-	0.0	Berggreen et al., 1988
<i>Acartia tonsa</i>	Calanoid	<i>Isochrysis galbana</i>	92	5	-	0.0	Berggreen et al., 1988
<i>Acartia tonsa</i>	Calanoid	<i>Isochrysis galbana</i>	85	5	-	0.0	Berggreen et al., 1988
<i>Acartia tonsa</i>	Calanoid	<i>Isochrysis galbana</i>	161	5	-	0.2	Berggreen et al., 1988
<i>Acartia tonsa</i>	Calanoid	<i>Isochrysis galbana</i>	207	5	-	0.8	Berggreen et al., 1988
<i>Acartia tonsa</i>	Calanoid	<i>Isochrysis galbana</i>	192	5	-	1.3	Berggreen et al., 1988
<i>Acartia tonsa</i>	Calanoid	<i>Isochrysis galbana</i>	290	5	-	1.6	Berggreen et al., 1988
<i>Acartia tonsa</i>	Calanoid	<i>Isochrysis galbana</i>	265	5	-	2.2	Berggreen et al., 1988
<i>Acartia tonsa</i>	Calanoid	<i>Isochrysis galbana</i>	270	5	-	2.9	Berggreen et al., 1988
<i>Acartia tonsa</i>	Calanoid	<i>Isochrysis galbana</i>	238	5	-	3.8	Berggreen et al., 1988
<i>Acartia tonsa</i>	Calanoid	<i>Isochrysis galbana</i>	311	5	-	2.9	Berggreen et al., 1988
<i>Acartia tonsa</i>	Calanoid	<i>Isochrysis galbana</i>	386	5	-	7.0	Berggreen et al., 1988
<i>Acartia tonsa</i>	Calanoid	<i>Dunaliella tertiolecta</i>	70	6	-	0.1	Berggreen et al., 1988
<i>Acartia tonsa</i>	Calanoid	<i>Dunaliella tertiolecta</i>	85	6	-	0.4	Berggreen et al., 1988
<i>Acartia tonsa</i>	Calanoid	<i>Dunaliella tertiolecta</i>	121	6	-	1.6	Berggreen et al., 1988
<i>Acartia tonsa</i>	Calanoid	<i>Dunaliella tertiolecta</i>	135	6	-	1.4	Berggreen et al., 1988
<i>Acartia tonsa</i>	Calanoid	<i>Dunaliella tertiolecta</i>	161	6	-	1.5	Berggreen et al., 1988
<i>Acartia tonsa</i>	Calanoid	<i>Dunaliella tertiolecta</i>	238	6	-	1.6	Berggreen et al., 1988
<i>Acartia tonsa</i>	Calanoid	<i>Rhodomonas baltica</i>	67	7	-	0.0	Berggreen et al., 1988
<i>Acartia tonsa</i>	Calanoid	<i>Rhodomonas baltica</i>	91	7	-	0.0	Berggreen et al., 1988
<i>Acartia tonsa</i>	Calanoid	<i>Rhodomonas baltica</i>	84	7	-	0.0	Berggreen et al., 1988
<i>Acartia tonsa</i>	Calanoid	<i>Rhodomonas baltica</i>	104	7	-	0.1	Berggreen et al., 1988
<i>Acartia tonsa</i>	Calanoid	<i>Rhodomonas baltica</i>	120	7	-	0.1	Berggreen et al., 1988
<i>Acartia tonsa</i>	Calanoid	<i>Rhodomonas baltica</i>	134	7	-	0.1	Berggreen et al., 1988
<i>Acartia tonsa</i>	Calanoid	<i>Rhodomonas baltica</i>	163	7	-	0.1	Berggreen et al., 1988
<i>Acartia tonsa</i>	Calanoid	<i>Rhodomonas baltica</i>	188	7	-	0.7	Berggreen et al., 1988
<i>Acartia tonsa</i>	Calanoid	<i>Rhodomonas baltica</i>	206	7	-	0.7	Berggreen et al., 1988
<i>Acartia tonsa</i>	Calanoid	<i>Rhodomonas baltica</i>	238	7	-	1.5	Berggreen et al., 1988
<i>Acartia tonsa</i>	Calanoid	<i>Rhodomonas baltica</i>	256	7	-	1.9	Berggreen et al., 1988
<i>Acartia tonsa</i>	Calanoid	<i>Rhodomonas baltica</i>	261	7	-	2.9	Berggreen et al., 1988
<i>Acartia tonsa</i>	Calanoid	<i>Rhodomonas baltica</i>	296	7	-	9.1	Berggreen et al., 1988
<i>Acartia tonsa</i>	Calanoid	<i>Rhodomonas baltica</i>	381	7	-	4.1	Berggreen et al., 1988
<i>Acartia tonsa</i>	Calanoid	<i>Rhodomonas baltica</i>	318	7	-	1.2	Berggreen et al., 1988
<i>Acartia tonsa</i>	Calanoid	<i>Amphidinium carterae</i>	135	9	-	0.4	Berggreen et al., 1988
<i>Acartia tonsa</i>	Calanoid	<i>Amphidinium carterae</i>	189	9	-	1.2	Berggreen et al., 1988
<i>Acartia tonsa</i>	Calanoid	<i>Amphidinium carterae</i>	206	9	-	1.0	Berggreen et al., 1988
<i>Acartia tonsa</i>	Calanoid	<i>Amphidinium carterae</i>	264	9	-	2.2	Berggreen et al., 1988
<i>Acartia tonsa</i>	Calanoid	<i>Amphidinium carterae</i>	289	9	-	2.5	Berggreen et al., 1988
<i>Acartia tonsa</i>	Calanoid	<i>Amphidinium carterae</i>	234	9	-	3.2	Berggreen et al., 1988
<i>Acartia tonsa</i>	Calanoid	<i>Amphidinium carterae</i>	260	9	-	3.4	Berggreen et al., 1988
<i>Acartia tonsa</i>	Calanoid	<i>Amphidinium carterae</i>	304	9	-	6.5	Berggreen et al., 1988
<i>Acartia tonsa</i>	Calanoid	<i>Amphidinium carterae</i>	376	9	-	15.4	Berggreen et al., 1988
<i>Acartia tonsa</i>	Calanoid	<i>Thalassiosira weissflogii</i>	94	14	-	0.0	Berggreen et al., 1988
<i>Acartia tonsa</i>	Calanoid	<i>Thalassiosira weissflogii</i>	69	14	-	0.0	Berggreen et al., 1988

APPENDIX II Continued.

Copepod species	Order	Prey species	Copepod ESD (μm)	Prey ESD (μm)	Maximum ingestion rate ($\mu\text{g C cop}^{-1} \text{d}^{-1}$)	Maximum clearance rate ($\text{mL cop}^{-1} \text{d}^{-1}$)	Source
<i>Acartia tonsa</i>	Calanoid	<i>Thalassiosira weissflogii</i>	119	14	-	0.2	Berggreen et al., 1988
<i>Acartia tonsa</i>	Calanoid	<i>Thalassiosira weissflogii</i>	133	14	-	0.3	Berggreen et al., 1988
<i>Acartia tonsa</i>	Calanoid	<i>Thalassiosira weissflogii</i>	162	14	-	0.9	Berggreen et al., 1988
<i>Acartia tonsa</i>	Calanoid	<i>Thalassiosira weissflogii</i>	191	14	-	2.8	Berggreen et al., 1988
<i>Acartia tonsa</i>	Calanoid	<i>Thalassiosira weissflogii</i>	213	14	-	6.7	Berggreen et al., 1988
<i>Acartia tonsa</i>	Calanoid	<i>Thalassiosira weissflogii</i>	247	14	-	11.5	Berggreen et al., 1988
<i>Acartia tonsa</i>	Calanoid	<i>Thalassiosira weissflogii</i>	270	14	-	16.9	Berggreen et al., 1988
<i>Acartia tonsa</i>	Calanoid	<i>Thalassiosira weissflogii</i>	270	14	-	22.1	Berggreen et al., 1988
<i>Acartia tonsa</i>	Calanoid	<i>Thalassiosira weissflogii</i>	296	14	-	19.9	Berggreen et al., 1988
<i>Acartia tonsa</i>	Calanoid	<i>Thalassiosira weissflogii</i>	319	14	-	17.8	Berggreen et al., 1988
<i>Acartia tonsa</i>	Calanoid	<i>Thalassiosira weissflogii</i>	383	14	-	59.0	Berggreen et al., 1988
<i>Acartia tonsa</i>	Calanoid	<i>Scropsiella faroense</i>	207	19	-	0.9	Berggreen et al., 1988
<i>Acartia tonsa</i>	Calanoid	<i>Scropsiella faroense</i>	189	19	-	2.1	Berggreen et al., 1988
<i>Acartia tonsa</i>	Calanoid	<i>Scropsiella faroense</i>	238	19	-	5.2	Berggreen et al., 1988
<i>Acartia tonsa</i>	Calanoid	<i>Scropsiella faroense</i>	260	19	-	5.2	Berggreen et al., 1988
<i>Acartia tonsa</i>	Calanoid	<i>Scropsiella faroense</i>	306	19	-	5.8	Berggreen et al., 1988
<i>Acartia tonsa</i>	Calanoid	<i>Scropsiella faroense</i>	260	19	-	8.9	Berggreen et al., 1988
<i>Acartia tonsa</i>	Calanoid	<i>Scropsiella faroense</i>	290	19	-	11.0	Berggreen et al., 1988
<i>Acartia tonsa</i>	Calanoid	<i>Scropsiella faroense</i>	372	19	-	11.6	Berggreen et al., 1988
<i>Acartia tonsa</i>	Calanoid	<i>Gymnodinium splendens</i>	189	71	-	3.7	Berggreen et al., 1988
<i>Acartia tonsa</i>	Calanoid	<i>Gymnodinium splendens</i>	203	71	-	4.6	Berggreen et al., 1988
<i>Acartia tonsa</i>	Calanoid	<i>Gymnodinium splendens</i>	238	71	-	3.9	Berggreen et al., 1988
<i>Acartia tonsa</i>	Calanoid	<i>Gymnodinium splendens</i>	265	71	-	9.4	Berggreen et al., 1988
<i>Acartia tonsa</i>	Calanoid	<i>Gymnodinium splendens</i>	311	71	-	18.0	Berggreen et al., 1988
<i>Acartia tonsa</i>	Calanoid	<i>Gymnodinium splendens</i>	386	71	-	27.7	Berggreen et al., 1988
<i>Clausocalanus lividus</i>	Calanoid	<i>Rhodomonas salina</i>	650	7	-	6.6	Isari and Saiz, 2011
<i>Clausocalanus lividus</i>	Calanoid	<i>Heterocapsa sp</i>	650	14	-	33.1	Isari and Saiz, 2011
<i>Clausocalanus lividus</i>	Calanoid	<i>Thalassiosira Weissflogii</i>	583	14	-	70.1	Isari and Saiz, 2011
<i>Clausocalanus lividus</i>	Calanoid	<i>Gymnodinium sp</i>	543	16	-	43.1	Isari and Saiz, 2011
<i>Clausocalanus lividus</i>	Calanoid	<i>Oxhyrris marina</i>	681	17	-	109.1	Isari and Saiz, 2011
<i>Clausocalanus lividus</i>	Calanoid	<i>Strombidium sulcatum</i>	660	28	-	189.2	Isari and Saiz, 2011
<i>Acartia grani naupli</i>	Calanoid	<i>Heterocapsa sp</i>	86	13	-	0.2	Henriksen et al., 2007
<i>Acartia grani naupli</i>	Calanoid	<i>Thalassiosira weissflogii</i>	86	14	-	0.2	Henriksen et al., 2007
<i>Acartia grani F</i>	Calanoid	<i>Alexandrium minutum</i>	19.3	441	7	-	Costa and Fernández, 2002
<i>Acartia grani F</i>	Calanoid	<i>Gyrodinium corsicum</i>	12.6	441	3	-	Costa and Fernández, 2002
<i>Acartia grani F</i>	Calanoid	<i>Rhodomonas baltica</i>	7.5	441	2	-	Costa and Fernández, 2002
<i>Oithona nana</i>	Cyclopoid	<i>Acartia nauplii</i>	154	80	-	13.5	Lampitt, 1978
<i>Oithona nana</i>	Cyclopoid	<i>Acartia nauplii</i>	149	80	-	15.6	Lampitt, 1978
<i>Oithona nana</i>	Cyclopoid	<i>Isochysis galbana</i>	154	-	-	0.3	Lampitt and Gamble, 1982
<i>Oithona nana</i>	Cyclopoid	<i>Dunaliella euchlora</i>	154	-	-	0.2	Lampitt and Gamble, 1982
<i>Oithona nana</i>	Cyclopoid	<i>Chricosphaera elongata</i>	154	-	-	1.0	Lampitt and Gamble, 1982
<i>Oithona nana</i>	Cyclopoid	<i>Thalassiosira weissflogii</i>	154	-	-	0.2	Lampitt and Gamble, 1982
<i>Oithona nana</i>	Cyclopoid	<i>Prorocentrum micans</i>	154	-	-	0.4	Lampitt and Gamble, 1982
<i>Oithona nana</i>	Cyclopoid	<i>Acartia clausi nauplii N1</i>	154	-	-	15.6	Lampitt and Gamble, 1982
<i>Oithona nana</i>	Cyclopoid	<i>Calanus finmarchicus N1</i>	154	-	-	4.6	Lampitt and Gamble, 1982
<i>Oithona nana</i>	Cyclopoid	<i>Calanus finmarchicus NII</i>	154	-	-	2.0	Lampitt and Gamble, 1982
<i>Oithona davisae</i>	Cyclopoid	<i>Oxhyrris marina</i>	158	17	-	2.3	Saiz et al., 2003
<i>Oithona davisae</i>	Cyclopoid	<i>Oxhyrris marina</i>	144	17	-	1.0	Kjørboe, 2008b
<i>Oithona davisae</i>	Cyclopoid	<i>Heterocapsa sp</i>	80	13	-	0.1	Henriksen et al., 2007
<i>Oithona similis</i>	Cyclopoid	<i>Various flagellates and ciliates</i>	179	11	-	1.3	Nakamura and Turner, 1997
<i>Oithona similis</i>	Cyclopoid	<i>Various flagellates and ciliates</i>	179	15	-	1.0	Nakamura and Turner, 1997
<i>Oithona similis</i>	Cyclopoid	<i>Various flagellates and ciliates</i>	179	9	-	2.4	Nakamura and Turner, 1997
<i>Oithona similis</i>	Cyclopoid	<i>Various flagellates and ciliates</i>	179	14	-	1.1	Nakamura and Turner, 1997
<i>Oithona similis</i>	Cyclopoid	<i>Various flagellates and ciliates</i>	179	15	-	1.4	Nakamura and Turner, 1997
<i>Oithona similis</i>	Cyclopoid	<i>Various flagellates and ciliates</i>	179	22	-	1.9	Nakamura and Turner, 1997
<i>Oithona similis</i>	Cyclopoid	<i>Various flagellates and ciliates</i>	179	27	-	3.7	Nakamura and Turner, 1997
<i>Oithona similis</i>	Cyclopoid	<i>Various flagellates and ciliates</i>	179	30	-	5.5	Nakamura and Turner, 1997
<i>Oithona similis</i>	Cyclopoid	<i>Prorocentrum micans</i>	179	11	0.2	3.0	Drits and Semenova, 1984
<i>Oithona similis</i>	Cyclopoid	<i>Peridinium trochoideum</i>	179	11	0.2	3.6	Drits and Semenova, 1984
<i>Oithona similis</i>	Cyclopoid	<i>Platymonas viridis</i>	179	11	0.3	3.3	Drits and Semenova, 1984
<i>Oithona davisae</i>	Cyclopoid	<i>Oxhyrris marina</i>	112	17	0.0	0.2	Almeda et al., 2010
<i>Oithona davisae</i>	Cyclopoid	<i>Oxhyrris marina</i>	114	17	0.0	0.2	Almeda et al., 2010
<i>Oithona davisae</i>	Cyclopoid	<i>Oxhyrris marina</i>	117	17	0.0	0.2	Almeda et al., 2010
<i>Oithona davisae</i>	Cyclopoid	<i>Oxhyrris marina</i>	133	17	0.0	0.3	Almeda et al., 2010
<i>Oithona davisae</i>	Cyclopoid	<i>Oxhyrris marina</i>	155	17	0.1	0.6	Almeda et al., 2010
<i>Oithona davisae</i>	Cyclopoid	<i>Oxhyrris marina</i>	158	17	0.1	4.8	Zamora-Terol and Saiz 2013
<i>Euterpina acutifrons</i>	Harpacticoid	<i>Alexandrium minutum</i>	281	19	3.5	-	Costa and Fernández, 2002
<i>Euterpina acutifrons</i>	Harpacticoid	<i>Gyrodinium corsicum</i>	281	13	2.4	-	Costa and Fernández, 2002
<i>Euterpina acutifrons</i>	Harpacticoid	<i>Rhodomonas baltica</i>	281	8	1.9	-	Costa and Fernández, 2002
<i>Euterpina acutifrons</i>	Harpacticoid	<i>plastic beads</i>	281	5	-	17.2	Sautour and Castel, 1993
<i>Euterpina acutifrons</i>	Harpacticoid	<i>Isochrysis galbana</i>	281	5	-	5.9	Sautour and Castel, 1993
<i>Euterpina acutifrons</i>	Harpacticoid	<i>Chaetoceros calcitrans</i>	281	11	-	4.4	Sautour and Castel, 1993
<i>Euterpina acutifrons</i>	Harpacticoid	<i>Skeletonema costatum</i>	281	6	-	11.5	Sautour and Castel, 1993
<i>Euterpina acutifrons</i>	Harpacticoid	<i>Prorocentrum micans</i>	281	28	-	5.3	Nassogne, 1970
<i>Euterpina acutifrons</i>	Harpacticoid	<i>Platymonas succia</i>	281	8	-	13.2	Nassogne, 1970
<i>Euterpina acutifrons</i>	Harpacticoid	<i>Gymnodinium sp</i>	281	8	-	2.6	Nassogne, 1970
<i>Oncaea mediterranea</i>	Poecilostomatoida	<i>Gymnodinium nelsoni</i>	85	42	0.0	0.1	Paffenhöfer, 1993
<i>Oncaea mediterranea</i>	Poecilostomatoida	<i>Gymnodinium nelsoni</i>	112	42	0.0	0.2	Paffenhöfer, 1993
<i>Oncaea mediterranea</i>	Poecilostomatoida	<i>Gymnodinium nelsoni</i>	125	42	0.0	0.2	Paffenhöfer, 1993
<i>Oncaea mediterranea</i>	Poecilostomatoida	<i>Gymnodinium nelsoni</i>	135	42	0.1	0.5	Paffenhöfer, 1993
<i>Oncaea mediterranea</i>	Poecilostomatoida	<i>Gymnodinium nelsoni</i>	171	42	0.2	1.0	Paffenhöfer, 1993
<i>Oncaea mediterranea</i>	Poecilostomatoida	<i>Gymnodinium nelsoni</i>	193	42	0.2	0.9	Paffenhöfer, 1993
<i>Oncaea mediterranea</i>	Poecilostomatoida	<i>Gymnodinium nelsoni</i>	209	42	0.5	2.2	Paffenhöfer, 1993
<i>Oncaea mediterranea</i>	Poecilostomatoida	<i>Gymnodinium nelsoni</i>	247	42	0.2	1.0	Paffenhöfer, 1993
<i>Oncaea mediterranea</i>	Poecilostomatoida	<i>Gymnodinium nelsoni</i>	248	42	0.2	1.1	Paffenhöfer, 1993
<i>Temora longicornis</i>	Calanoid	<i>Rhodomonas salina</i>	435	6	2.1	10.4	this study, type II model fit

APPENDIX II Continued.

Copepod species	Order	Prey species	Copepod ESD (μm)	Prey ESD (μm)	Maximum ingestion rate ($\mu\text{g C cop}^{-1} \text{d}^{-1}$)	Maximum clearance rate ($\text{mL cop}^{-1} \text{d}^{-1}$)	Source
<i>Temora longicornis</i>	Calanoid	<i>Thalassiosira weissflogii</i>	518	9	3.3	28.9	this study, type II model fit
<i>Temora longicornis</i>	Calanoid	<i>Prorocentrum minimum</i>	560	10	9.9	23.4	this study, type II model fit
<i>Temora longicornis</i>	Calanoid	<i>Oxyhris marina</i>	526	11	8.2	39.4	this study, type II model fit
<i>Temora longicornis</i>	Calanoid	<i>Heterocapsa triquetra</i>	584	12	6.4	35.6	this study, type II model fit
<i>Temora longicornis</i>	Calanoid	<i>Scrippsiella trochoidea</i>	523	16	2.7	40.0	this study, type II model fit
<i>Temora longicornis</i>	Calanoid	<i>Protoceratium reticulatum</i>	506	23	5.4	85.1	this study, type II model fit
<i>Temora longicornis</i>	Calanoid	<i>Lingulodinium polyedrum</i>	554	24	5.3	146.9	this study, type II model fit
<i>Temora longicornis</i>	Calanoid	<i>Akashiwo sanguinea</i>	552	33	2.3	243.9	this study, type II model fit
<i>Temora longicornis</i>	Calanoid	<i>Akashiwo sanguinea</i>	486	42	1.6	231.8	this study, type II model fit
<i>Temora longicornis</i>	Calanoid	<i>Coscinodiscus radiatus</i>	481	58	2.3	154.6	this study, type II model fit
<i>Temora longicornis</i>	Calanoid	<i>Rhodomonas salina</i>	435	6	1.8	7.2	this study, type III model fit
<i>Temora longicornis</i>	Calanoid	<i>Thalassiosira weissflogii</i>	518	9	2.6	21.1	this study, type III model fit
<i>Temora longicornis</i>	Calanoid	<i>Prorocentrum minimum</i>	560	10	5.4	21.5	this study, type III model fit
<i>Temora longicornis</i>	Calanoid	<i>Oxyhris marina</i>	526	11	5.6	32.8	this study, type III model fit
<i>Temora longicornis</i>	Calanoid	<i>Heterocapsa triquetra</i>	584	12	4.8	27.6	this study, type III model fit
<i>Temora longicornis</i>	Calanoid	<i>Scrippsiella trochoidea</i>	523	16	2.5	25.0	this study, type III model fit
<i>Temora longicornis</i>	Calanoid	<i>Protoceratium reticulatum</i>	506	23	4.6	59.2	this study, type III model fit
<i>Temora longicornis</i>	Calanoid	<i>Lingulodinium polyedrum</i>	554	24	5.0	88.7	this study, type III model fit
<i>Temora longicornis</i>	Calanoid	<i>Akashiwo sanguinea</i>	552	33	2.2	120.8	this study, type III model fit
<i>Temora longicornis</i>	Calanoid	<i>Akashiwo sanguinea</i>	486	42	1.6	110.1	this study, type III model fit
<i>Temora longicornis</i>	Calanoid	<i>Coscinodiscus radiatus</i>	481	58	2.2	96.8	this study, type III model fit